DISSERTATION FOR THE DEGREE OF DOCTOR OF PHILOSOPHY (PHD)

Role of ion channels in CAR-T cells

by Ghofrane Medyouni

Supervisor: Dr. Hajdu Péter Béla

UNIVERSITY OF DEBRECEN

DOCTORAL SCHOOL OF MOLECULAR MEDICINE

DEBRECEN, 2025

DISSERTATION FOR THE DEGREE OF DOCTOR OF PHILOSOPHY (PHD)

Role of ion channels in CAR-T cells

by Ghofrane Medyouni

Supervisor: Dr. Hajdu Péter Béla

UNIVERSITY OF DEBRECEN

DOCTORAL SCHOOL OF MOLECULAR MEDICINE

DEBRECEN, 2025

TABLE OF CONTENTS

LIST OF ABBREVIATIONS

AB2: Secondary antibody
AP-1: Activator protein 1
APC: Antigen presenting cell
BBIR: Biotin binding immune receptor
BK: Big conductance
CaM: Calmodulin
CAR: Chimeric antigen receptor
CHO: Chinese hamster ovary
CRAC: Ca^{2+} release activated Ca^{2+} channel
CRS: Cytokine release syndrome
CTL: Cytotoxic T lymphocytes
DAG: Diacylglycerol
EDTA: Ethylenediaminetetraacetic acid
EBIO: 1-Ethylbenzimidazolinone
ER: Endoplasmic reticulum
FBS: Foetal bovine serum
FITC: Fluorescein isothiocyanate
GK: Conductance of K^+
HEK: Human embryonic Kidney
HNSCC: Head and neck squamous cell carcinoma
IFN: Interferon
IK: Intermediate conductance
IL: Interleukin
IP3: 1,4,5 inositol triphosphate
IP3R: 1,4,5 inositol triphosphate receptor
IS: Immune synapse
KCa: Calcium gated potassium channel
Kir: Inwardly rectifying potassium channel
Kv: Voltage gated potassium channel
MDSC: Myeloid derived suppressor cells
MHC: Major histocompatibility complex
NF: Nuclear factor
NFAT: Nuclear factor of activated T-cells
NK: Natural killer cell
NT: Non-transduced cells
P: Pore loop
PBL: Peripheral blood lymphocyte
PBMCs: Peripheral blood mononuclear cells

pA: picoampere
PD: pore-forming domain
PIP2: phosphatidylinositol-4,5-biphosphate
PKC: Protein Kinase C
PLC: Phospholipase C
ROS: Reactive oxygen species
ScFv: Single-chain variable fragment
SCID: Severe combined immunodeficiency
SF: Selectivity filter
SK: Small-conductance $Ca2^{+}$-activated K^{+} channels
SOC: Store operated channels
SUPRA: Split, universal programmable
TAA: Tumor associated antigens
TAM: Tumor associated macrophages
T_{CM}: Central memory T cell
TCR: T cell receptor
T_{EM}: Effector memory T cells
TIL: Tumor infiltrating lymphocytes
TM: Transmembrane domain
TME: Tumor microenvironment
TNF: Tumor necrosis factor
TRAM-34: 1-[(2-Chlorophenyl)diphenylmethyl]-1H-pyrazole
TCR: T cell receptor
TRUCK T: T redirected for antigen-unrestricted cytokine-initiated killing
VSD: Voltage-sensitive domain

LIST OF FIGURES

1 INTRODUCTION

The immune system is a marvel of biological complexity, an impressive network of cells, molecules and signals building up a solid vital system. Unfortunately, this system fails to survey the abnormal growth of cells in the case of cancer. In parallel, potassium channels control different physiological functions in human T lymphocytes. These membrane proteins essentially maintain a negative resting membrane potential through K^+ efflux, which regulates Ca^{2+} signaling for T-cell proliferation and cytokine generation. Kv1.3, KCa3.1 and CRAC channels the most important channels in the Ca^{2+}-activated pathway.

Despite the shared scientific goal of deciphering one of the leading causes of death, cancer, only a small niche of studies is bridging the gap between immunology and biophysics.

This presented dissertation attempts to extend our knowledge of the relationship between ion channels and CAR T-cells, which are crucial player in a very promising immunotherapy in the fight against cancer. The challenges that this therapy still faces, despite the remarkable success, have prompted us to investigate a better understanding of its function through the analysis of the role of ion channels.

To do so, we created a cell model expressing third generation CARs and we investigated the role of Kv1.3 channel alone at first. Via this cell model, we studied the colocalization of the CAR and the Kv1.3 channel in standalone cells as well as in the synapse formed between Jurkat-CARs and targeted Raji CD19 $^+$ cells.

Furthermore, we enlarged this study by examining the role of Kv1.3, KCa3.1, CRAC channels in primary CAR-T cells against HER2 positive cancer cells. Using patch-clamp technique and calcium-imaging we reveal the biophysical properties of these channels. To our knowledge, no study reported on modelling CAR-T function by ion channels inhibitors. Therefore, we were curious to test these antagonists in the aim of overcoming the side-effects of this therapy as well as enhancing its efficacy. To thoroughly assess this, we performed functional assays that target either the blocking of the function or the movement of ion channels into the formed synapse.

Overall, the present study provides new insights into future clinical strategies.

2 LITERATURE REVIEW

2.1 Ion channels

Ion channels are widely expressed membrane proteins that form a hydrophilic pore in the cell membrane (including plasma membrane and intracellular organelle membranes), allowing the passage of various ions (Na^+, K^+, Ca^{2+}, Cl^-) according to their electrochemical gradient [1].The different behavior of ions channels (high rate, passive transport) versus thermo-dynamically uphill transport of pumps makes them distinguished entities. The ion movement control by the ions channels is essential for life. Several cellular functions are mediated by them such as immune responses , muscle contraction, pH regulation and cell cycle [2]. The classification of ions channels mostly relies on ion selectivity (e.g. Ca^{2+}, K^+, Cl^-, highly, mildly- or non-selective), ionic current direction (outward-, inward), gating mechanism (voltage-gated, signal-gated, ligand-gated, stretch-gated, etc.) [3]. In this study, K^+ and CRAC Ca^{2+} channels are our primary focus, and this will be covered in more detail below.

2.1.1 K^+ channel

More than 90 genes in the human genome code for principal subunits of K^+ channels forming a large family in both excitable and non-excitable cells. These proteins are implicated in several crucial biological processes like cellular signaling in the nervous system, regulation of cell volume, proliferation and activation of T cells, apoptosis and Ca^{2+} signaling [4, 5]. From a structure point of view, K^+ channels are composed of pore forming α-subunits with auxiliary β-subunits [6] [7]. K^+ channels can be categorized into 4 different subfamilies based on their subunit structure (Figure 1): (i) 6TM-segment (S1-S6) channels having one pore domain including voltage-gated K^+ channels (Kv),(ii) inwardly-rectifying K^+ (K_{ir}) regulated by intracellular factors permitting the movement of K^+ into the cell, (iii) two-pore, four TM segments K^+ channels (K_{2P}) which assemble as dimers and (iv) KCa Ca^{2+}-activated potassium channels 6/7 TM/1P [8, 9]. The selectivity of potassium channels is determined by a conserved sequence of amino acids referred to as the signature sequence T/SXGXGX located in the pore forming region [10]. The understanding of potassium channels' properties is essential for developing novel therapeutic agents targeting ion channels disorders [11].

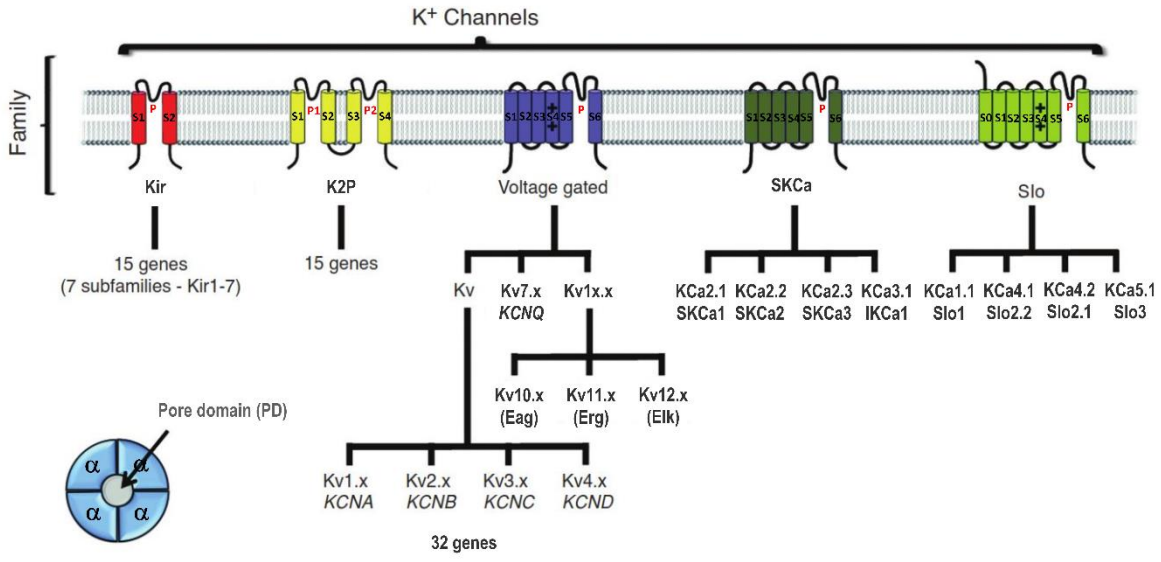

Figure 1. **Classification of potassium channels based on their subunit structure.** Kir**:** inward rectifier K^+ channels (2TM and 1P); K2P: background or leak K^+ channel (4TM and 2P); Voltage-gated K^+ channels (6TM and 1P); SKCa: Ca^{2+}-activated K^+ channels (6TM and 1P); and Slo: voltage- and Ca^{2+}-gated K^+ channels (6 or 7 TM and 1P). Four α-subunits assembling into a tetramer to form a functional K^+-conducting pore is represented in the inset bottom left. Image modified from [12].

2.1.2 Voltage-gated potassium channels (Kv)

Voltage-gated potassium channels form one of the largest and most diverse protein family, encoded by 40 genes in the human genome and divided into 12 subfamilies [13]. These subfamilies can be classified into three groups [14, 15]. The dominant group in this division is the Kv1 (Shaker-like channels) that includes 8 voltage-gated K^+ channels (Kv1.1-1.8) [16]. Kv channels consist of four α-subunits arranged as homotetramers or heterotetramers, each subunit contains six transmembrane α-helical segments (S1-S6). The voltage sensitivity is due to the voltage sensing domain (VSD) formed by the first 4 α-helices (S1-S4) due to the positively charged amino-acid residues in the S4, while selectivity is ensured by the region between S5 and S6 in the pore domain (PD) and the connecting pore loop (P) [17]. Kv channels have been thoroughly characterized. However, basic properties of Kv α-subunit channel can be modified by the different possibilities of heteromultimerization of α-subunits, their association with intracellular β-subunits or furthermore due to phosphorylation and dephosphorylation [18]. This molecular variety presents a challenge in terms of drug discovery, but it also offers the possibility to design specific modulators that bind to tissue-specific β-subunits or that differentiate between homotetramers or heterotetramers [19].

In our current study, our main focus is the Kv1.3 ion channel (Figure 2).It is in the plasma membrane, nuclear membrane, cis-Golgi apparatus membrane, and in the inner mitochondrial membrane [20]. Kv1.3 opens upon depolarization. One of the main distinctive properties of Kv1.3 channel is the P/C inactivation or also called slow inactivation which consists of a time-dependent inactivation that develops during repetitive or prolonged depolarization. This type involves conformational changes in the pore (P) and C-terminal region [21, 22].

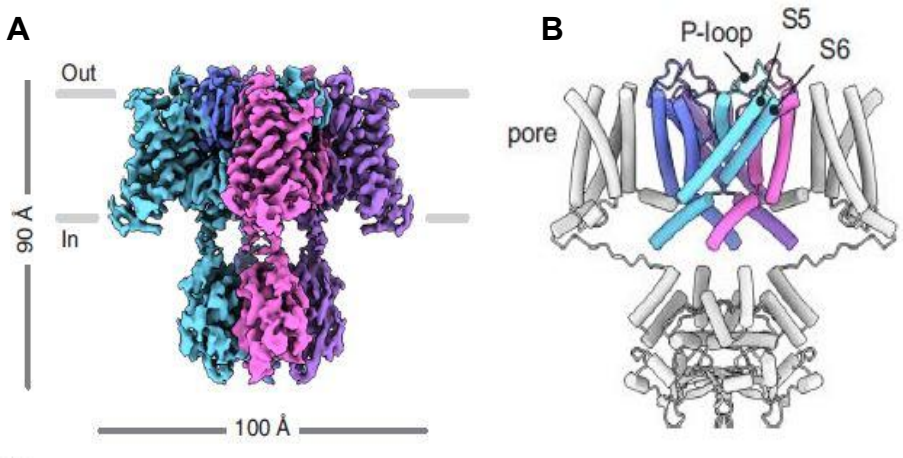

Figure 2**. Structure of human Kv1.3. (A)** Cryo-EM density map of human Kv1.3**. (B)**. The front and rear VSDs are omitted for clarity in B. Image cropped from figure1 of [23].

2.1.3 KCa: calcium activated potassium channels

Calcium activated potassium channels are widely expressed in variety of tissues such as muscles, neurons and immune cells [24]. As their name states, they require an intracellular calcium signal to function. According to their conductance, 3 categories has been identified: small conductance (SK) 2–25 pS (SK1, SK2, and SK3), which correspond to KCa2.1, KCa2.2, and KCa2.3 [25], intermediate conductance (IK) 25–100 pS [26] referred to as KCa3.1, SK4, or IK1, and large conductance with a range of 200–300 pS that are not only regulated by calcium signal but also voltage-dependent referred to as BK channels [27]. Besides the difference in conductance, these 3 classes differ significantly in terms of Ca^{2+} binding affinity and location. IK and SK channels have a high affinity of 0.1-0.4 µM and 0.3-0.75 µM, respectively [28, 29]. BK channels have a low affinity of 1-11 µM. The opening of the channel of IK and SK is modulated via a calmodulin-binding domain [30-32]. In this research study we are focused on KCa3.1 channel. The intermediated-conductance Ca^{2+}-activated K^+ channel KCa3.1 (KCNN4) is mostly distributed in blood cells, liver, lungs, placenta, endothelial and vascular cells [33, 34]. Unlike Kv channels, they do not respond to voltage changes but to the calcium binding to the calmodulin inducing channel opening [35]. In immune cells, KCa3.1 is

upregulated in activated cells compared to resting T cells [36]. It plays a crucial role in immunity and cancer that we will detail in other sections. According to its expression pattern, KCa3.1 modulators represents a therapeutic candidate for autoimmune diseases [37], blocking proliferation of smooth muscle cells and fibroblasts in atherosclerosis [38] and asthma [39].

2.1.4 CRAC channels

Calcium is considered one of the most important second messengers that modulate several physiological responses. Generally, the stimulation of cell surface receptors induces the production of 1,4,5-inositol triphosphate (IP_3) provoking the release of Ca^{2+} from the endoplasmic reticulum (ER) and inducing a calcium influx across the plasma membrane due to the activation of store-operated Ca^{2+}-entry via store-operated channels (SOCs) [40]. The Ca^{2+}release-activated Ca^{2+} (CRAC) channel known as a category of store-operated channels (SOCs) were the first to be studied using electrophysiological techniques. These channels have been well characterized in terms of biophysical properties and signaling pathways mainly in T lymphocytes because of the key role they play in their activation [41]. They are known by their low conductance, however high selectivity for Ca^{2+} [42]. The depletion of the ER store in the endoplasmic reticulum membrane is sensed by the STIM1, stromal interaction molecule 1, transmembrane protein with several EF-hand motif that sense the ER Ca^{2+} concentration identified as the Ca^{2+} ER sensor. STIM1 is localized primary in the ER membrane with a small fraction in the plasma membrane (Figure 3) [43]. After the calcium signal, this protein undergoes conformational changes, multimerizes and redistributes into discrete puncta near plasma membrane where it activates the pore-forming domain ORAI1 (also known as CRACM1) [44-46]. CRAC channels are considered as a powerful tool for the raise of cytosolic Ca^{2+}, which is directly linked to several cellular responses. Ca^{2+} increase stimulates gene expression, mitochondrial metabolism and cell growth and proliferation [47]. Multiple channelopathies are linked to abnormal CRAC channel activity resulting in severe combined immunodeficiency disease (SCID) [44], breast cancer [48] and allergy [49].

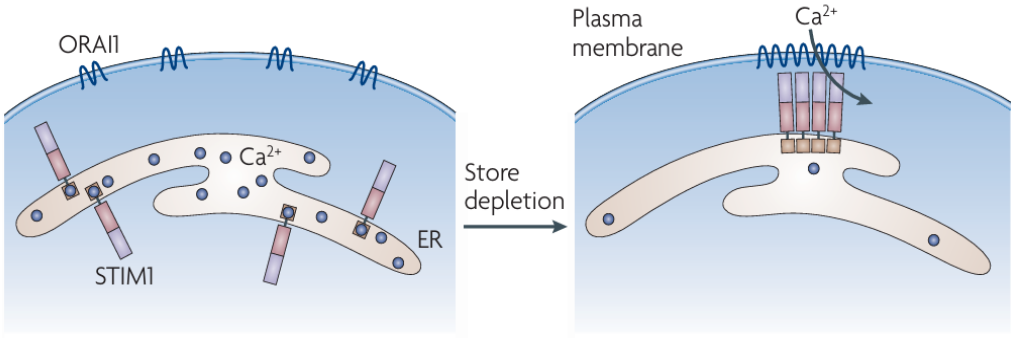

Figure 3: **Gating of Ca^{2+}release-activated Ca^{2+} CRAC channels (CRAC).** Upon stimulation via the increase of cytoplasmic calcium level, STIM-1 molecules oligomerize and migrate to the ER–plasma membrane junctions. At these sites, STIM1 captures diffusing ORAI1 channels. Interaction between the amino and carboxyl termini of ORAI1 with the CRAC activating domain (CAD) on STIM1 leads to CRAC channel opening. Image cropped from figure 2 of [43].

2.2.1 Brief review of the immune system

The immune system is one of the most fascinating networks in our body. There are two fundamental ways of defending against pathogens: the innate and the adaptive response. The first one uses cells like macrophages, monocytes, neutrophils, and natural killer cells. This response is also modulated via molecules such as the complement system and cytokines like interferons. Adaptive response requires the proliferation of antigen-specific T and B cells. Antigen-presenting cells (APCs) like dendritic cells and macrophages display the antigen to lymphocytes through a transmembrane protein complex called MHC (major histocompatibility complex). This will lead to cell activation, proliferation, and differentiation. The effector response could occur via antibodies released from the differentiated plasmocytes or direct cell elimination by T cytotoxic cells. The $CD4^+$ or helper T cells are considered as the ones orchestrating the immune response via the recognition of foreign antigens and activating cell-mediated responses. Naïve T cells ($CCR7^+/CD45RA^+$) that circulate in the bloodstream differentiate into lymphoblasts upon encountering a specific antigen, subsequently developing into effector T cells through a process of rapid clonal proliferation. After the clearance of the antigen, a considerable number of effector T cells undergo apoptosis; however, a minority differentiate into central memory T cells (T_{CM}, $CCR7^+/CD45RA^-$) and effector memory T cells (T_{EM}, $CCR7^{-/}CD45RA^-$). These cells are characterized by the lack of CD45RA cell surface phosphatase and the presence or absence of the CCR7 marker, respectively. Their primary function is to swiftly activate the adaptive immune system in response to repeated antigenic stimulation. The immune system reactions are complex and involve several parts. However,

they are a major target for therapeutic development against infections, tumors, and autoimmune diseases [50-52].

2.2.2 Role of Kv1.3 and KCa3.1 in calcium-activated signaling of T cells

In 1984, scientists detected the expression of voltage-gated K^+ channels in human T lymphocytes, which triggered the interest of immunologists to determine the role played by these proteins in the immune system [53, 54]. Upon these findings, the Kv channel was identified as Kv1.3 [55] . Later, several cells of innate and adaptive immune cells were found to express ion channels permitting the influx and/or efflux of ions across the plasma membrane or their release from the organelles, such as the ER, lysosomes, or mitochondria [56, 57]. Studies identified that patients having mutations affecting ion channels, like inherited channelopathies, lead to immunodeficiency and autoimmune diseases [58]. Pharmacological experiments with ion channel inhibitors also revealed the important ionic signaling in lymphocyte development and accurate innate and adaptive responses. The activation of T cells results from a cascade of events starting with the interaction between the TCR in T cells and the antigen-presenting MHC of APCs (*Figure 4*). TCR engagement leads to the induction of the signal transduction pathway. One of the most important pathways lies in the recruitment of PLCγ1, a phospholipase, which gets activated and cleaves phosphatidylinositol 4,5-bisphosphate (PIP_2) into diacylglycerol (DAG) and inositol 1,4,5-triphosphate (IP_3). IP_3 binds to its receptor in the membrane of the ER (IP_3R), which induces the release of the stored Ca^{2+}. The depletion of the ER is sensed by the STIM1 molecule, which will oligomerize with ORAI1 channel to establish functional store-operated calcium release–activated Ca^2 (CRAC) channels. The intracellular Ca^{2+} level rises, provoking the activation of the phosphatase calcineurin. This enzyme dephosphorylates the nuclear factor of activated T-cells (NFAT) in the cytosol, leading to the activation and translocation to the nucleus. Other nuclear factors, such as NF-kB, can be activated via DAG and Ca^{2+} in a protein kinase C (PKC)-dependent manner. These stimuli could also modulate activator protein 1 (AP-1). NF-κB, NFAT, and AP-1 transcription factors regulate gene expression that orchestrate T cell proliferation and differentiation. It is important to mention that 75% of activation-regulated genes of T cells are Ca^{2+}-dependent through the plasma membrane via CRAC channels. Studies showed that the decrease in Ca^{2+} levels prevents T cell activation and proliferation [59-63]. This essential Ca^{2+} influx, considered as crucial for

T cell activation, must be counter-balanced by K^+ efflux maintained by Kv1.3 and KCa3.1 in order to avoid excessive depolarization of the plasma membrane [64-66] .

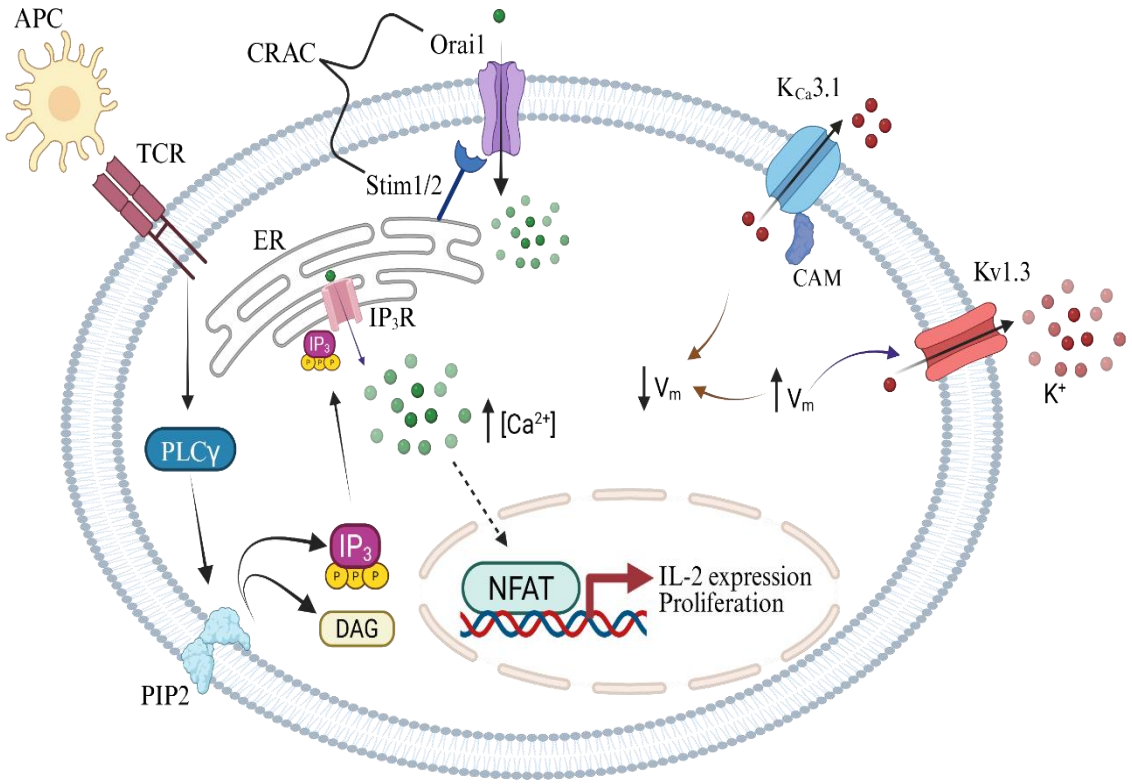

Figure 4**: Role of ion channels in T cell activation.** Upon binding between an antigen presenting cell (APC) and the T-cell receptor (TCR), PIP2 is cleaved generating second messenger IP3 and DAG via the activation of phospholipase C-γ (PLC-γ) signaling cascade. IP3 stimulates the IP3-receptor located in endoplasmic reticulum (ER) provoking the release of Ca^{2+} into cytosol. Depletion of Ca^{2+} in ER mobilizes Stim 1 and 2 which dimerize and activate the ORAI1 subunits of CRAC channel causing Ca^{2+} entry through cell membrane. The increase of the cytosolic free $Ca^{2+}$and the membrane depolarization (↑Vm) open the Ca^{2+}-activated KCa3.1 and voltage-gated Kv1.3 channels, respectively. The K^+ efflux through Kv1.3 and KCa3.1 counterbalances the depolarization effect caused by Ca^{2+} influx and repolarizes the membrane potential (↓Vm) thereby maintaining the driving force for further Ca^{2+} entry. Ca^{2+} signal regulates gene expression (e.g., IL-2 expression) leading to cell proliferation and effector functions through a series of signaling molecules. Image complied in BioRender.

Single-cell patch-clamp technique reported the differential channel expression of T cells depending on the cell type, state of activation, and differentiation.Resting T cells are characterized by a low expression of both K^+ channels; nevertheless, this expression is upregulated upon antigen engagement and activation as it is illustrated in Figure 5.

Memory T cells T_{CM} (long-lived central memory) and T_{EM} (effector-memory) formed during an immune response, present a distinguished K^+ channel expression pattern. 300 Kv1.3 channels per cell, along with 10-20 KCa3.1 channels, are present in quiescent human T_{CM} and T_{EM}. Consequent to cell activation, T_{CM} upregulates KCa3.1 when turning into T_{CM} effectors, while T_{EM} upregulates Kv1.3 when turning into T_{EM} effectors [67, 68]

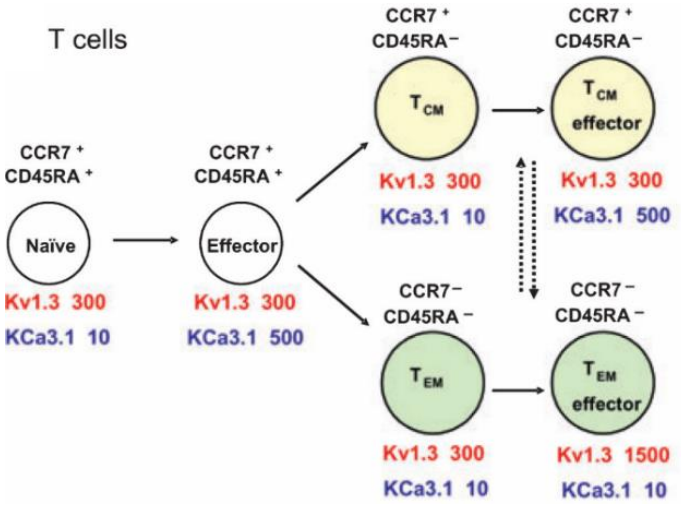

Figure 5: **Changes in K^+ channel expression during T cell activation.** The average number of functional Kv1.3 and KCa3.1 channels in individual $CD4^+$or $CD8^+$ human T cells isolated from peripheral blood and stained with antibodies specific to CCR7 and CD45RA. Naive ($CCR7^+CD45RA^+$), central memory TCM ($CCR7^+CD45RA^-$) and effector memory TEM ($CCR7^-CD45RA^-$). Image cropped from [65].

2.3 Ion channels and the tumor microenvironment

Previous studies showed that in the case of head-and-neck squamous cell carcinoma (HNSCC), K^+ currents measured from circulating T cells obtained from patients and healthy donors were similar. In contrast, Kv1.3 currents measured in biopsy-derived tumor infiltrating lymphocytes (TILs) are significantly lower. The function of these cells is altered since they stop proliferating and producing cytokines (Ki67 and granzymes). On the other hand, peripheral $CD8^+$ cells fail to upregulate the Ca^{2+} sensor calmodulin (CaM) causing a suppression of KCa3.1 function. This could lead to a limited ability of $CD8^+$ cells to infiltrate the tumor site. The use of KCa3.1 activator 1-EBIO restored the function of this ion channel and the migratory capacity of $CD8^+$ cells, hence the use of ion channel modulators could serve as therapeutic tool [69].

In addition to the fact that cancer is defined by the uncontrolled proliferation of tumor cells , it became obvious during the last few years that the environment in which these cells are proliferating referred to as tumor microenvironment (TME), plays a crucial role in tumor

development [70]. The TME is characterized by the presence of several cell types such as T and B cells, NK cells, myeloid derived suppressor cells (MDSC), dendritic cells and their surrounding stroma. One of the hallmarks of the TME is the suppressive feature that limits the infiltration of immune cells mainly CTL (cytotoxic T cells) and NK, impairs the function of anti-tumor immune response favoring the activation of suppressive cells such as Treg cells and MDSC [71]. Alongside the cell composition, the mediators secreted in the TME sparked the interest of the scientific community encouraging them to investigate this part. Blay et al gave evidence to the increase of adenosine levels, a metabolite resulting from the degradation of ATP, in the TME. In fact, as a response to pathophysiological conditions e.g. inflammation, ischemia, hypoxia, the concentration of adenosine, originally low at unstressed tissues rises to induce cellular responses aiming to restore the tissues homeostasis. However, the persistence of this high concentration can turn to the opposite effect and cause an immunosuppressive niche. This has been further investigated demonstrating the elevated adenosine effect on T cells function via the engagement of adenosine A2A receptors [72, 73]. It is important to note that adenosine release is also triggered by genetic changes that occur during tumorigenesis [74]. Numerous types of neoplasia upregulated the expression and activity of CD73, the main adenosine generating enzyme ecto-5′-nucleotidase, responsible for dephosphorylating AMP to adenosine [75]. The mechanism responsible for the suppressive property of adenosine was analyzed by Conforti's lab. The findings of this study clearly illustrate the involvement of ion channels in this loop. Adenosine selectively inhibits KCa3.1 but not Kv1.3 and TRPM7 in activated human T-cells, mediated by the cAMP/PKAI signaling pathway as adenylyl-cyclase and PKAI inhibition prevented the effect of adenosine on KCa3.1. Comparable results to adenosine inhibition on cell migration were obtained via the blockade of KCa3.1 by TRAM-34. In addition, adenosine suppresses IL2 secretion throughout KCa3.1 inhibition [76]. All this data strengthens the possibility of targeting ion channels as a therapeutic anti-cancer tool.

2.4 Modulators of Kv1.3 and KCa3.1

2.4.1 Kv1.3 modulators

Kv1.3 and KCa3.1 significantly contribute to several physiological and pathophysiological functions; therefore, they are one of the main potential pharmacological targets. Specific blockers of Kv1.3 channel are suggested for the treatment of autoimmune diseases and neuroinflammatory disorders since this channel is upregulated in T_{EM} and in activated microglia. Numerous attempts have been made to investigate and optimize the pharmacological properties of Kv1.3 blockers lately [77, 78]. Nevertheless the diverse assembly of the subunits

of Kv1.x channel subunits and their expression pattern represents a challenge in drug discovery [79]. Venom-derived peptide toxins and small organic molecules are the two large groups that block Kv1.3 channels. The small molecules bind to the central cavity located under the selectivity filter of the channel. Because of their small size (800 Da) it interacts with the binding site which is similar to the subtypes of the Kv1.3 channel resulting in a low affinity [79, 80].To date, PAP-1 is the most promising small molecule inhibiting Kv1.3 channel with 23-fold selectivity over other reported molecules [81]. The second group of blockers is the peptide toxins isolated from animal venom (scorpions, spiders, snakes). These molecules' size range is of 3-4 kDa and are characterized by a larger interacting surface. Therefore, they could have high selectivity, which minimize the potential side effects [82]. There are currently 350 entries in the Kalium database, which is a compilation of natural peptides that inhibit K^+ channels with varying affinities ranging from pM to µM concentration [83]. In our study we used one of the toxins derived from scorpion (KTxs family) referred to as Vm24 (α- KTx 23.1) isolated from the venom of the *Vaejovis mexicanus smithi* scorpion, Vm24 inhibits Kv1.3 channels of human T cells with high affinity (K_d = 2.9 pM), >1500-fold selectivity over other reported ion channels [84] . One of the hallmarks of this toxin is the suppression of the proliferation (*in vitro)* and Ca^{2+} signaling which makes it an exceptional candidate for the treatment of autoimmune diseases such as psoriasis, multiple sclerosis and rheumatoid arthritis[85]. Other studies reported the negative effect on the secretion of the pro-inflammatory cytokines IFN-γ and TNF and the anti-inflammatory cytokines IL-4, IL-5, IL-9, IL-10, and IL-13 [86]. Since Kv1.3 channel is typically targeted for inhibition, there are very few activators in the literature such as ceramides [87] .

2.4.2 KCa3.1 modulators

Pharmacological modulation of the human intermediate conductance calcium-activated potassium channel, KCa3.1, has gained significant attention in the last decade particularly due to its high relevance in the treatment of several malignancies [88]. Out of the small molecule inhibitors TRAM-34 (IC_{50}=20 nM), clotrimazole (IC_{50}=70-250 nM), senicapoc (IC_{50}=11nM) were proved to be the most potent and highest specificity. All of these listed inhibitors bind to the inner portion of the pore [89, 90]. Subsequently, TRAM-34 has been investigated intensively *in vitro* and *in vivo* by other scientists and proved to be a very promising molecule with less side effects than the previously reported drugs [91]. It has been reported that the blockage of KCa3.1 channel inhibits the progression of human endometrial cancer [92] and may serve as novel immunosuppressive strategy to prevent the rejection of kidney allograft

[93]. Besides the inhibitors of these channels, several activators are developed. The first one was reported back in 1996 known as 1-ethyl-2-benzimidazolinone (1-EBIO), belonging to the family of benzimidazolones [94]. Recently new drugs has been designed resembling 1-EBIO [95], but with a higher affinity reaching to nanomolar range such as oxime NS309 [96]. In this dissertation we used only the inhibitor TRAM-34 molecule.

2.5 The localization of Kv1.3 in the immunological synapse

The concept of the immunological synapse (IS) has shifted in recent years from a junction between the T cell and their antigen on the target cell or the antigen presenting cell to a whole dynamic reorganization of proteins and membrane domains into the IS. The distance between the two cells forming the IS varies between 15 nm at their closest to 100 nm. This region of contact was later on named the synaptic cleft [97, 98]. In the early stages of IS formation, the Ca^{2+}influx induces T cell "rounding" [99] as well as morphological changes such as the translocation of the mitochondria to the plasma membrane at the synapse supporting the Ca^{2+}influx [100]. The increase of the Ca^{2+} level upon TCR-antigen binding through the CRAC channels cause the phosphorylation of ERM proteins (ezrin, radixin and moesin) resulting in the detachment of the actin cytoskeleton from membrane proteins [101]. Other findings reported the enrichment of the lymphocyte function-associated antigen 1 in the periphery and TCR/CD3, CD28, and CD2 membrane proteins in the center of the supramolecular activation clusters, as well as the selective accumulation of cytosolic protein talin in the periphery, Lck and PKCθ in the center of the IS [102-104].

Due to the important role of the ion channels explained above in the Ca^{2+}-activated pathway (*Figure 4*), the localization of the ion channels upon the IS formation was studied. Several results reported the accumulation of ion channels in the IS [105, 106]. For the first time, a study from our laboratory gave proof to the redistribution of Kv1.3 channels into the IS formed between a cytotoxic T cell (CTL) and its target, where it formed clusters in the membrane of CTL cells (Figure 6) [107].The role of the Kv1.3 channel was highlighted furthermore via performing functional assays targeting the trafficking of it into the IS. The antibody-based crosslinking of Kv1.3 channels, leads to the immobilization of these proteins, affects the Ca^{2+}-response, hence the downstream Ca^{2+}-dependent pathway [108]. This clearly opens the possibility of modulating the T cell response via ion channels.

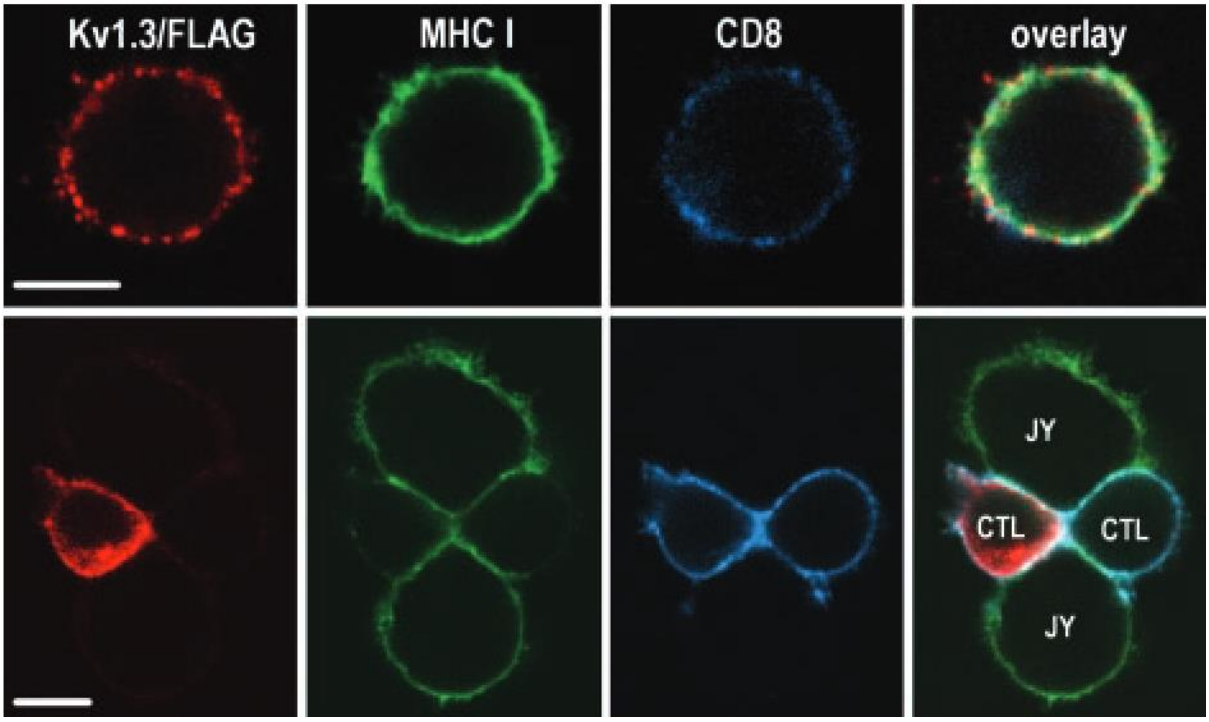

Figure 6 **:Distribution of the Kv1.3 /FLAG in the IS. Kv1.3/FLAG** (red: anti-FLAG followed by Alexa Fluor 546-RAMIG), MHC class I (green: X-FITC-W632), and CD8 (Alexa Fluor 647-anti-CD8) molecules in a standalone CTL (top) and CTL-JY target cell conjugates (Bottom). (scale bar, 5μm) [107].

2.6 CAR T cell therapy

2.6.1 CAR structure and evolution

Back in the 1960s, scientists figured out that our immune cells can fight against cancer and from that point on, immunotherapy started to develop [109]. Chimeric Antigen Receptor (CAR) was introduced to T cells mainly but not exclusively. Structurally, CARs are composed of 4 parts: 1) an extracellular part that serves as a recognition domain, 2) the hinge (spacer), 3) the transmembrane domain and 4) an intracellular part that plays essential role in the signaling pathway (as illustrated in Figure 7). During the development of the CAR T cell therapy, the genetically engineered receptor underwent a multi-stage refinement process resulting in 5 different generations to date. The first generation of CAR is composed of a fusion of proteins containing single-chain variable fragment (scFv) derived from an antibody, which functions as the extracellular antigen-binding domain associated with an intracellular part made up of costimulatory domains typically CD3 ζ. To enhance CAR T cell activity and persistence in the patient, costimulatory domains were added in addition of CD3 ζ in the second generation such as CD28 or 4-1BB. In the third generation, second costimulatory domains were introduced to improve CAR T cell activation, proliferation and anti-tumor activity. Clinical research

demonstrated that the second and third generations gave rise to significant improvements in the treatment of hematological cancers. In contrast, solid tumor treatment still faces a lot of limitations due to the suppressive tumor microenvironment and insufficient T cell infiltration. Hence, there was an urge to optimize the design introducing suitable modifications in the fourth generation [110, 111]. These cells are called T cells redirected for universal cytokine-mediated killing (TRUCK-T), "Armored CAR-T cells" or the fourth-generation [112] [113]. In this design, CAR T cells produce cytokines that serve as an additional signal to maintain a sustained T cell response [114]. As this therapy is continually under improvement, the fifth generation is currently in active development. Previous generations of CAR T cells were able to recognize one specific antigen on the targeted cell referred to as conventional or monovalent cells. In the latest model of this therapy, CARs went beyond conventional by incorporating additional structures to recognize more than one antigen or low antigen expression. The fifth generations are called universal CAR cells. These cells use a third-party sort of mechanism: the BBIR (biotin-binding immune receptor) CAR and the SUPRA (split, universal, programmable) CAR (as illustrated in Figure 7). The SUPRA CAR system consists of zipCAR: an engineered CAR-T cell receptor that contains a leucine zipper at the extracellular end, as well as an intracellular signaling domain. The zipFv is an antigen-binding fragment that also contains a complementary leucine zipper that enables it to selectively bind to zipCAR. On the other hand, BBIR CAR T cells (known as Bi-specific Biotin-binding Immune Receptor CAR T cells) target molecules that are biotinylated giving greater flexibility and safety [115, 116]. Overall, the CAR configuration shows significant variation across each generation. Further trials are in active research phases.

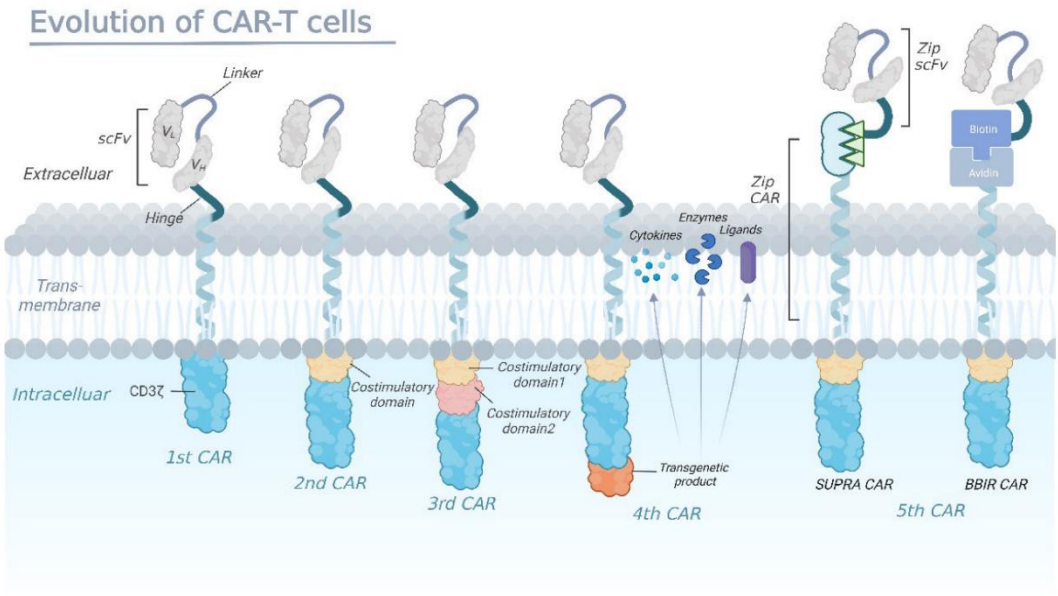

Figure 7:**The evolution of chimeric antigen receptors (CAR)-T cells** [120].

2.6.2 CAR T cells manufacturing

The effectiveness of CAR-T cell therapies relies on efficient cell manufacturing, which influences product safety, efficacy, and the accessibility for patients. Autologous CAR T production starts with isolating the peripheral blood mononuclear cells (PBMC) collected from whole blood (Figure 8) of the patient or more commonly through leukapheresis [117]. Because of the diversity of T cell types such as $CD8^+$cytotoxic T cells, $CD4^+$ helper cells: Th1, Th2, Th17, $CD4^+$ Treg cells, the selection of the initial cell population is a critical factor in the manufacturing process of CAR-T cells [118]. Density gradient centrifugation or elutriation is frequently utilized to eliminate undesirable contaminating cells, including granulocytes, red blood cells, and platelets [117]. CAR T cells are activated via the direct binding to the antigen in MHC independent-manner [119]. Therefore, CAR T cells function does not require the CD4 or CD8 molecules as co-receptors. Early research on CAR T cells immunotherapy proved the advantage of selective enrichment of $CD8^+$ T cells to enhance the cytotoxicity [120]. Nevertheless, $CD4^+$ helper T cells are essential for facilitating the effector functions, expansion, and longevity of $CD8^+$ T cells [121]**.** Studies have demonstrated that the presence of $CD4^+$ T cells within the tumor microenvironment enhances the recruitment, proliferation, and activity of $CD8^+$cytotoxic T cells [122]. Preclinical studies are highly suggested to determine the adequate CD4:CD8 ratio in more complex manufacturing approach [123]. Collected T cells are, in a second step, activated *ex vivo* through 3 distinct signals. Firstly, the typical antigen-specific binding by stimulating the epsilon subunit of the TCR/CD3 complex. The second, costimulatory signal is provided by activating the CD28 membrane protein. Third, is the cytokine signal,

considered crucial to fulfil the T cell activation [124, 125] . For that, T cells are grown in the presence of IL-2, IL-7, and IL-15 cytokines. Cytokine cocktail is used to manipulate T cell phenotype [126, 127]. Following activation, CAR genes are introduced to the cells by viral or non-viral delivery methods. Both retroviral and lentiviral methods have been recognized as safe and efficient [128]. Recently, T cells have been genetically modified via CRISPR-Cas9 technique. Engineering the next generation of CAR T cells with CRISPR-Cas9 gene editing seems to be very promising. Thanks to the flexibility, precision and effectiveness of this method, several limitations could be defeated. Recent studies demonstrated that the modulation of cytokine production through this method potentiates CAR T-cell function and reduces toxicity [129].

As a final step of CAR T cell production, the successfully transduced cells are cultivated in bioreactors to meet the required dose then administrated to the patient [130].The *ex vivo* expansion of T cells duration varies according to different protocols but usually takes up to 1-2 weeks from cell activation [131].

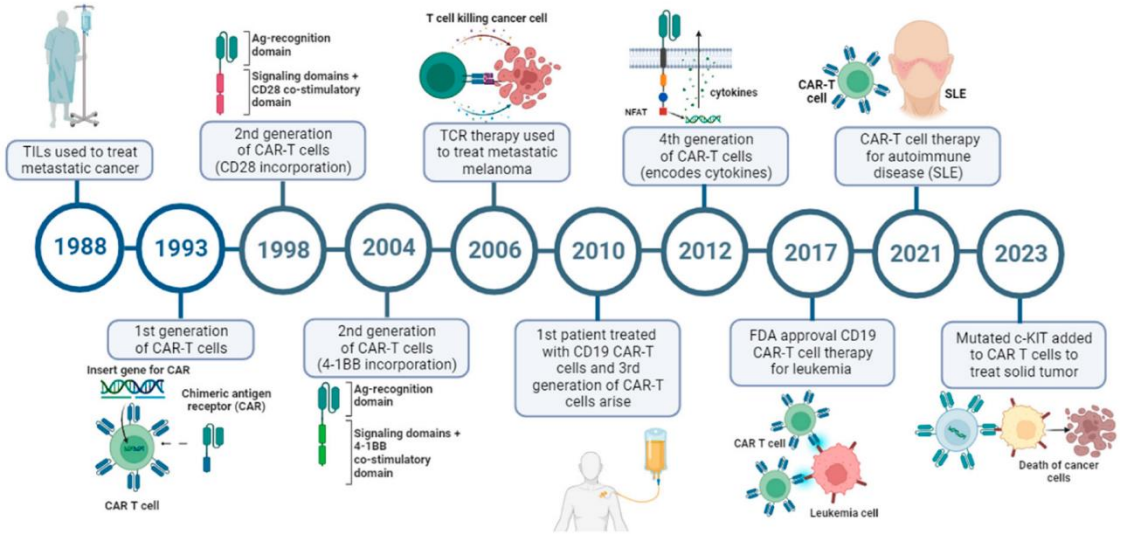

Figure 8: **Timeline of CAR-T cell therapy history**. The key milestones from the first TIL treatment of metastatic cancer to the newest CAR-T cell therapy application. (This figure was created using BioRender.com) [109].

2.7 CAR cells clinical application and limitations

2.7.1 CAR T cells targeting cancer

Several noteworthy breakthroughs of clinical applications of CAR T therapy are achieved in hematological malignancies. The first reported significant response was by Steven Rosenberg and James Kochenderfer where they managed to treat a patient with chemo refractory follicular

lymphoma (FL) using CD19 CD28ζ CAR-T cells, resulting in dramatic regression of tumor infiltration [132].Further clinical trial was led by Carl June and David Porter from Upenn where they reinfused CD19-specific 4-1BBζ CAR T cells to a patient with refractory CLL [133]. To date, FDA approved CD19-specific and BCMA-specific CAR T therapies like Kymriah® (tisagenlecleucel), Tecartus® (brexucabtageneautoleucel), Abecma® (Idecabtagene vicleucel), Breyanzi® (lisocabtagene maraleucel), and Yescarta® (axicabtagene ciloleucel) [134]. These notable achievements in hematological cancers paved the path for application in, however, it is a more complex challenge to be resolved compared to non-solid disorders. One of the most remarkable CAR-T cell therapy drugs is HER2-CAR T, which is able to reduce the human ovarian cancer growth [135]. Other studies by Zhou et al demonstrated that the use of MUC28z CAR-T cells in the case of triple negative breast cancer decrease the tumor proliferation and boost the production of Granzyme B, IFN-γ, and other types of cytokines and chemokines secreted by Th1 essential for the anti-tumor response [136]. Other promising under development CAR-T cells were produced for prostate, pancreatic, gastric, lung, liver and colorectal cancer [137-140]. Targeting solid tumors using CAR T cell therapy has been intensively explored in order to overcome the several challenges that the patients face. One of barriers of the effectiveness of this therapy is the heterogenicity of tumor associated antigens (TAA) of solid tumors since they are as well expressed by healthy tissues as well and their level of antigen expression differs from a tumor location to another [141]. New strategies are evolving to solve this problem by engineering a chimeric antigen receptor including two or more antigens recognition domains or by the co-expression of several CARs on a single T cell [142]. Another main limitation is the poor ability for CAR T cells to penetrate tumor tissues [143]. Tumor cells employ several escaping mechanisms such as downregulating adhesion molecules expression as well as chemokine secretion [144, 145]. Regional administration is shown to be more effective than the systematic when the site of tumors are restricted[146]. Another important challenge is the immunosuppressive character of TME. Unlike hematological malignancies, solid tumors sites are strongly infiltrated by different cell types that support tumor progression like myeloid-derived suppressor cells (MDSCs), Treg cells and tumor-associated macrophages (TAMs) [147]. The side effects of the treatment present an obstacle as well to overpass (Figure *9*). A common occurrence after CAR T therapy in oncology is hypogammaglobulinemia [152, 153], infections with grade 3-5 reported in clinical trials of commercial agents for 5-33% of patients [154-157] and severe cytokine release syndrome (CRS) associated with the massive T cell expansion *in vivo* [158].

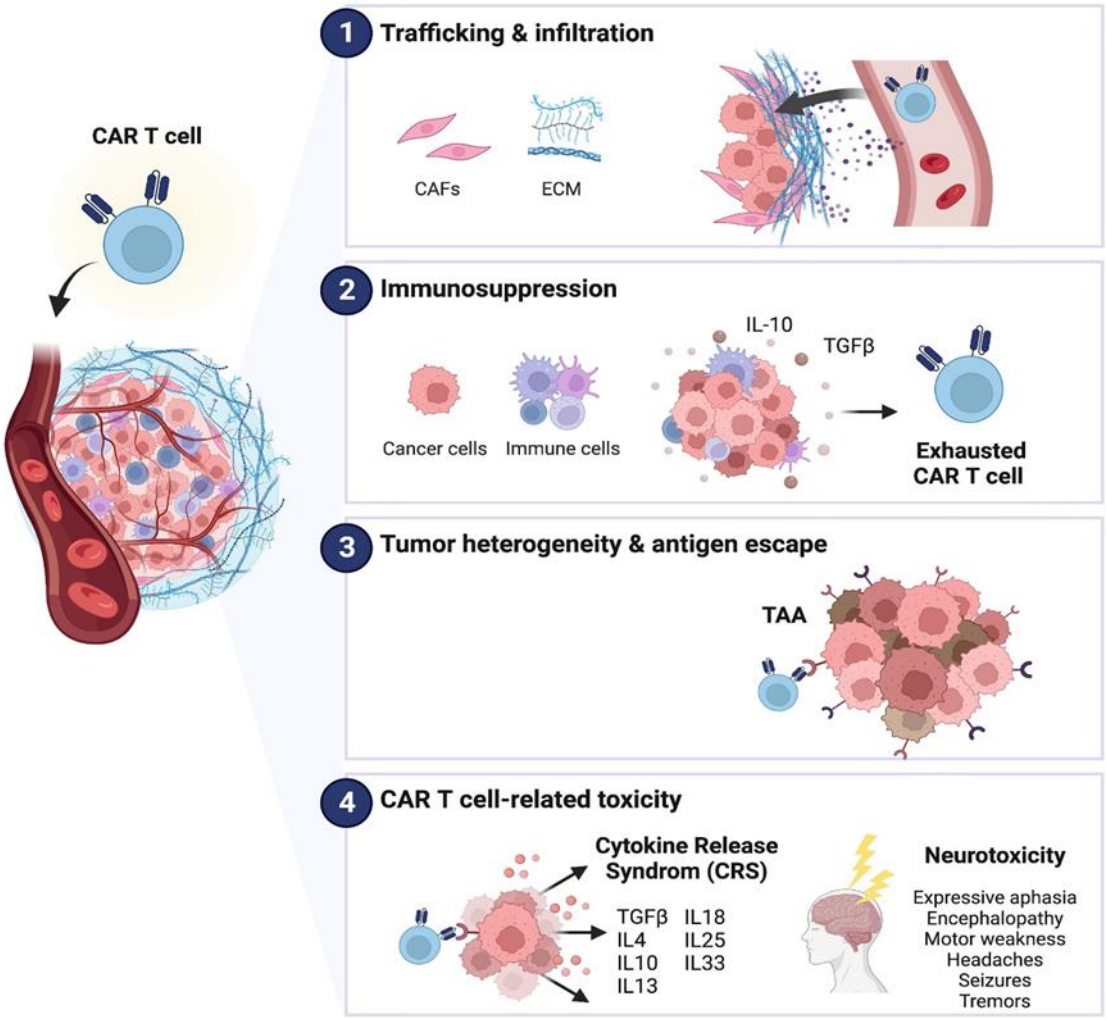

Figure 9: **CAR T cell therapy limitations**. Image cropped from [159].

2.7.2 Other clinical applications of CAR T cell therapy

Beyond the application of CAR T cell therapy in cancer; this technology is applied in multiple other areas. The potential of anti-CD19 CAR T cell therapy to deplete B cells, as in the case of acute lymphoblastic leukemia [148] B cell lymphoma [149], paved the way to its implementation in treating autoimmune diseases. Results from a lupus mouse model treated by $CD8^+$ CAR T cell only, or a mix of $CD4^+$ and $CD8^+$ cells demonstrated an efficient reduction of tissue-resident B cells and improvement of mouse survival [150, 151]. Recent studies of patients with autoimmune diseases strongly support the usage of CAR T cells. The case report of the 20-year-old woman with severe refractory SLE is a remarkable example [152]. The infusion of these genetically engineered cells was additionally well-tolerated in systemic

sclerosis [153-155], myasthenia gravis [156] and refractory anti-synthetase syndrome [156, 157]. So far, research on the safety considerations for CAR T cell therapy in autoimmune diseases have reported lower toxicity experience from CRS and ICANS compared with patients receiving this therapy for cancer [158, 159]. For selective targeting of autoreactive B cells, scientists designed a chimeric immunoreceptor expressing the pathogenic autoantigen in the extracellular part. A preclinical trial in the case of the myasthenia gravis model, MuSK-CAAR was as efficient as anti-CAR T cells without causing B cell depletion [160].

3 AIMS

CAR-T cell immunotherapy has proven to be a promising treatment for blood cancer patients. However, several challenges need to be overcome. It has been previously described that K^+ channels play an important role in T cell effector function. To date, no study reported about the role of ion channels in CAR-T cells. In the thesis we studied the role of CAR-T cell K^+ channels in target cell elimination with two distinct approaches. They were the following:

3.1 To unveil the functional role of Kv1.3 channel localization in Jurkat-CAR cells

The first step was the establishment of anti-CD19 CAR expressing Jurkat cell line (Jurkat-CAR) and validate the functionality of the CAR using Calcein-Red AM based killing assay. Second, we analyzed the biophysical properties of Kv1.3 in Jurkat-CAR cells and assessed the localization of Kv1.3 channel in standalone and target cell engaged Jurkat-CAR cells. Since the channel is involved in the Ca^{2+}-dependent activation pathway, our aim was to monitor the Ca^{2+}-response during the synapse formation between the target cells and Jurkat-CARs. To reveal the Kv1.3 channel role we unveiled the influence of Kv1.3 channel immobilization via antibody-crosslinking on the Jurkat-CAR Ca^{2+}-response and target cell killing.

3.2 Determine the expression and role of K^+ channels in anti-HER2 3rd generation CAR-T cells

In the second part of the study, we aim to characterize the expression of Kv1.3 and KCa3.1 in $CD4^+$and $CD8^+$ third-generation anti-HER2 CAR-T cells and evaluate the Ca^{2+}-response of $CD4^+$and $CD8^+$ of CAR T cells. Using ion channel inhibitors, we tested the role of ion channels in the killing potential of CAR-T cells.

4 MATERIALS AN D METHODS

4.1 Cell culture

4.1.1 HEK 293T cell line

HEK-293T packaging cells were cultured in a DMEM medium (Sigma-Aldrich Ltd., Hungary), which contained 10% FBS, 1 mM Na-pyruvate, and 200 units of penicillin/streptomycin. Cells were maintained at 37 °C in a humid atmosphere of 5% CO_2 and 95% air. Cells were passaged thrice in a week following 2-5 minutes incubation in 0.05% trypsin-EDTA solution.

4.1.2 Jurkat and Raji cell line

Jurkat and Raji cell lines were cultured in a RPMI medium (Sigma-Aldrich Ltd., Hungary) supplemented with 10% FBS, 1 mM Na-pyruvate, and 200 units of penicillin/streptomycin. Cells were maintained at 37 °C in a humid atmosphere of 5% CO_2 and 95% air. Cells were passaged thrice in a week.

4.1.3 MDA-MB-468, N87 and JIMT-1 cell lines

The triple-negative human breast cancer cell line MDA-MB-468 (abbreviated MDA in the text), and N87 human gastric cancer cell lines were purchased from the American Type Culture Collection (ATCC, Manassas, VA, USA). The cells were cultured in Dulbecco's Modified Eagle Medium (DMEM) supplemented with 2 mmol/l GlutaMAX and 10% Fetal Calf Serum (FCS) and antibiotics. The JIMT-1 human breast cancer cell line was established in the laboratory of Cancer Biology, University of Tampere, Finland [161]. These cells were cultured in a 1:1 ratio of Ham's F-12 and DMEM supplemented with 20% FCS, 300 U/L insulin, 2 mmol/l GlutaMAX, and antibiotics. MDA.ffLuc, JIMT-1.ffLuc, and N87.ffLuc were generated by single-cell cloning of the MDA-MB-468, JIMT-1, and N87 cell lines, respectively, after transduction with a retrovirus encoding eGFP.ffLUC to express an enhanced green fluorescent protein/firefly luciferase fusion gene [162].

4.1.4 Isolation of primary human T cells

The experiments were carried out on human samples by the Declaration of Helsinki and approved by the Regional and Institutional Committee for Research Ethics (RKEB.5378/2019). To isolate human T cells, human peripheral blood mononuclear cells were isolated by Ficoll gradient centrifugation and stimulated in non-tissue culture 24-well plates precoated with 1 µg/mL OKT3 (Thermo Fischer, Waltham, MA, USA) and anti-CD28 (R&D Systems, Minneapolis, MN, USA) antibodies. On day 2, human interleukin-7 (IL-7; 10 ng/mL) and human interleukin-15 (IL-15; 5 ng/mL) (Miltenyi Biotec, Bergisch Gladbach, Germany) were added to cultures. The primary human T cells were cultured in the RPMI (Roswell Park

Memorial Institute) medium supplemented with 2 mmol/l GlutaMAX and 10% FCS and antibiotics. All the cells and cell lines were maintained in a humidified atmosphere containing 5% CO_2, 95% air at 37 °C and were routinely checked for the absence of mycoplasma contamination by PCR.

4.2 Retroviral transduction

4.2.1 Anti-CD19 Jurkat-CARs

To generate Jurkat-CAR cells, 2 $\times 10^6$ cells of HEK293T were plated in a 10 cm petri dish with 10 ml of DMEM medium supplemented with 10% FBS. To proceed, the cells were required to adhere to the plate and reach 70-80% confluence. The plasmids used (described in the table and

Figure 10 below) were mixed and diluted in 500 µL of jetPRIME buffer followed by the addition of 20 µL of jetPRIME® reagent (Polyplus, Illkirch, France). The mixture was incubated for 10 min at room temperature. As a last step, the transfection mixture was added to plated HEK293T cells and incubated for 48 hours in a humidified atmosphere containing 5% CO_2, 95% air, at 37 °C.

Table 1: **Retroviral transduction plasmids**

Plasmid	Amount
pBMN-sGFP-CAR	4 µg
pBMN-empty vector	4 µg
psPAX2	3 µg
VSVG	3 µg

Figure 10: pBMN-sGFP-CD19-CAR construct. Image cropped from [175].

For evaluating the transfection efficacy HEK293T transfected cells with pBMN-sGFP-CAR were checked under the microscope for GFP positivity. Later, the viral supernatant was removed from the HEK293T cells and collected, filtered using a 0.45 µm filter then added to the target

Jurkat cells, along with the polybrene (10 µg/ml). Transduced Jurkat cells (Jurkat-CAR) were incubated for 48 hours at 37 °C in a humidified atmosphere of 5% CO_2, 95% air. The retroviral transduction efficiency was evaluated using flow cytometry along with non-transduced Jurkat cells (NT-Jurkat) as a control for the cells transduced with pBMN-sGFP-CAR. For the cells transduced with the empty vector of pBMN (Jurkat-PBMN cells), the antibiotic selection marker was utilized to select transduction positive cells.

4.2.2 CAR-T cells

For the generation of HER2-specific CAR T cells , the RD114-pseudotyped retroviral particles were generated by transient transfection of the HEK 293T cells with the HER2-specific CAR-encoding pSFG retroviral vectors, the Peg-Pam-e plasmid coding MoMLV gag-pol, and the pMax.RD114 plasmid using jetPRIME transfection reagent (Polyplus, Illkirch, France)[163, 164]. The construct of the HER2-CAR is illustrated in Figure 11.

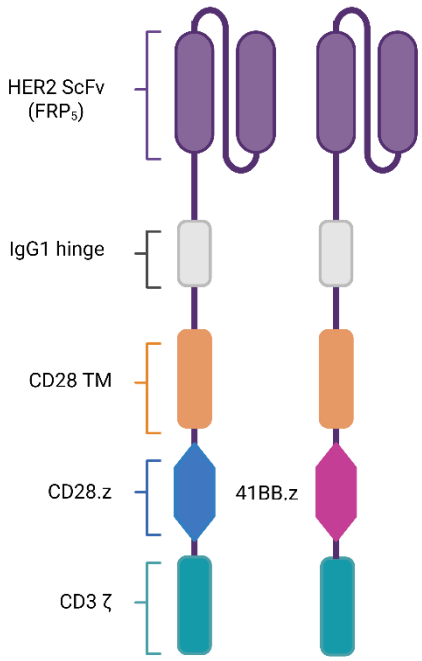

Figure 11: **HER2-CAR construct**. Image complied in BioRender.

After human T cell isolation (detailed above), T cells were transduced with retroviral particles on RetroNectin-coated (Takara, Kusatsu, Japan) plates on day 3 in the presence of IL-7 (10 ng/mL) and IL-15 (5 ng/mL). The expansion of the T cells was subsequently supported by IL-7 and IL-15. The OKT3/CD28-activated non-transduced (NT) T cells were expanded with IL-

7 and IL-15 using the same protocol. Following 48 h incubation, the cells were used for further experiments [162].

4.3 Anti-CD19 Jurkat-CARs sorting

To get a homogeneous cell population, we proceeded with cell sorting using cytoFLEX Flow cytometer using GFP as a marker for the CAR^+ cells. At first, the 10×10^6 of the transduced cells were centrifuged and washed with PBS then re-suspended into 1% FBS-PBS. Jurkat non-transduced cells were used as a negative control. After sorting, cells were centrifuged for 5 minutes, 300×g at RT then re-suspended in RPMI medium and placed in the incubator to grow at 37 °C in a humidified environment of 5% CO_2, 95% air, with the RPMI medium replenished every 2 days. Results were analyzed with FCS Express 6 software.

4.4 Single-cell electrophysiology

4.4.1 Patch-clamp electrophysiology conditions

Whole-cell currents were measured using patch-clamp technique in voltage-clamp configuration following standard protocols [165]. All recordings were performed using Axopatch 200B amplifier connected to a personnel computer with Axon Digidata 1440 digitizer and for data acquisition and analysis, Clampex 10.7 software was used (Molecular Devices, Sunnyvale, CA, USA). Micropipettes were pulled from GC150F-7.5 borosilicate capillaries (Harvard Apparatus, Kent, UK) with a tip resistance ranging 3-5 MΩ in the bath solution. Recordings were performed at room temperature (20-25 °C).

4.4.2 Solutions

The intracellular and extracellular solutions were prepared according to table 2 and table 3 below. The osmolarity of the intracellular solution used to measure Kv1.3 and KCa3.1 currents of CAR T cells was 290–310 mOsm with 1μM free Ca^{2+} concentration, and ~295 mOsm for the one used for measuring Kv1.3 channel in Jurkat-CARs. pH of solutions was set before performing the experiments.

Table 2: Composition of extracellular/bath solution for patch-clamp recording

	Kv1.3	Kv1.3 and KCa3.1
NaCl (mM)	145	
KCl (mM)	5	5
$MgCl_2$ (mM)	1	1
$CaCl_2$ (mM)	2.5	2.5
Na-aspartate (mM)	-	145
Glucose (mM)	5.5	5.5
HEPES (mM)	10	10
pH	7.35	7.4

Table 3: Composition of intracellular/pipette solution for patch-clamp recording

	Kv1.3	Kv1.3 and KCa3.1
KF(mM)	140	-
$MgCl_2$ (mM)	2	2
$CaCl_2$ (mM)	1	8.5
K-aspartate (mM)	-	145
K_2EGTA (mM)	11	10
HEPES (mM)	10	10
pH	7.2	7.2

4.5 Voltage Protocols

4.5.1 Kv1.3 measurements of Jurkat-CARs

Jurkat-CARs were placed into cell culture 35 mm petri dishes. Kv1.3 currents were recorded in whole-cell configuration using the solutions listed above. The activation kinetics of the current were characterized by fitting the Hodgkin-Huxley (HH) model ($I(t)=I_a \times (1-\exp(-t/\tau_a))4+C$, where I_a is the amplitude of the activating current component; τ_a is the activation time constant

of the current; C: current at the beginning of the trace) to the rising phase of the current trace obtained by 15 ms long depolarization to +50 mV. The activation time constant characterizes the average of the time constants of a given cell upon three sequential depolarizations repeated every 15 s.

The inactivation kinetics of the current were characterized by fitting a single exponential function ($I(t) = I_0 \times \exp(-t/\tau_{in}) + C$, I_0: amplitude of the current, τ_{in}: inactivation time constant, C: the steady-state value of whole-cell current at the end of the pulse) to the decaying part of the current traces obtained by 2 s long depolarization to +40 mV from a holding potential of -120 mV. The inactivation time constant was determined as for the activation, except that pulses were delivered every 60 seconds.

The voltage dependence of steady-state activation was determined as follows. Jurkat-NT, Jurkat-CAR, and Jurkat-PBMN were held at -120 mV holding potential and depolarized to various test potentials ranging from -70 mV up to +50 mV in 10 mV steps at every 30 s. Peak whole-cell conductance (G(V)) at each test potential was calculated from the peak current (I_p) at test potential V and the K^+ reversal potential (E_r=−85 mV) using $G(V)=I_p/(V-E_r)$. The G(V) values were normalized for the maximum conductance and plotted as a function of test potential and the Boltzmann function was fitted to the data points: $G_N=1/(1+\exp[-(V-V_{½})/k]$, where G_N is the normalized conductance, V is the test potential, $V_{½}$ is the midpoint or half-maximal activation potential and k is the slope factor of the function.

4.5.2 Kv1.3 and KCa3.1 measurements of CAR-T cells

$CD3^+$ CAR/NT cells were plated onto a poly-l-lysine-coated 35 mm petri dish, while CD4 and CD8 CAR T and NT cells were adhered to a petri dish using the antibody adhesion protocol as described here [166]. The Kv1.3 and KCa3.1 currents in the CAR-T cells were measured in a whole-cell voltage-clamp configuration. The solutions used are described above. The currents were recorded by 200 ms ramp depolarization from −120 to + 50 mV from a holding potential of −70 mV at every 15 s. KCa3.1 conduction was defined as the ratio of the linear fraction of the macroscopic current slope and the slope of the voltage-ramp stimulus after subtraction of the leak current, $G_{KCa3\ 1}(nS) = I_{slope}\left(\frac{pA}{ms}\right) / V_{slope}\left(\frac{V}{ms}\right)$. The slope conductance was measured between −100 and −60 mV to avoid contamination by the Kv1.3 current. As for the Kv1.3 current, it was determined from the same ramp protocol at 50 mV after subtraction of the KCa3.1 current extrapolated by linear regression. The conductance for each channel type was normalized to whole-cell capacitance (which is proportional to the channel number per unit area) and was applied to define the membrane expression level.

4.6 Intracellular Ca^{2+} measurements

4.6.1 Ca^{2+} response of standalone Jurkat-CARs and CAR-T cells

To determine the effect of CAR expression on the CRAC-related Ca^{2+}-response, a FURA-2 Ca^{2+}-imaging technique was performed. For Jurkat-CARs, cells (Jurkat CAR/NT/PBMN) were plated onto poly-L-lysine coated glass bottom petri dishes. For CAR-T cells, cells were labeled using CD4-Alexa488 or CD8-Alexa488 (Biolegend, San Diego, CA, USA). Then, the cells were suspended in 10% BSA in PBS for 30 min on ice, then washed 2 times with PBS, then resuspended in phenol-red free media. Afterwards, CAR T cells were plated onto poly-L-lysine-coated glass bottom petri dishes as well and underwent the same procedure. To track the Ca^{2+} response, cells were loaded with 1 µM Fura 2-acetoxymethyl ester (Thermo Fisher Scientific, Budapest, Hungary) dissolved in DMSO and incubated for 30 min at 37 °C in phenol -Red free RPMI solution (Sigma-Aldrich Ltd., Budapest, Hungary), supplemented with 1% FBS, 2mM L-glutamine, 1mM Na-pyruvate and 200 units penicillin/streptomycin. Later, we washed the cells with 2 mM Ca^{2+} solution (see table 4 for the recipe of solutions) and placed them on a 37 °C stage of an inverted fluorescence microscope. Then, cells were perfused with 2 mM Ca^{2+} solution, 0 mM Ca^{2+} and then 1 µM thapsigargin (TG) (Thermo Fisher Scientific) containing 0 mM Ca^{2+} solution was applied to deplete the Ca^{2+} stores via passive release from the endoplasmic reticulum (ER). After store depletion, the addition of the extracellular 2 mM Ca^{2+} containing 1µM TG activated intracellular Ca^{2+} elevation through SOCE (store-operated calcium entry). Experiments with FURA-2 were done with an inverted NIKON ECLIPSE Ts2R microscope combined with a VisiChrome High-Speed Polychromator (Visitron Systems GmbH, Puchheim, Germany). FURA-2 dual excitation and emission were accomplished using 340 nm and 380 nm excitation filters and a 510 nm emission filter. Digital images (200 ms exposure) were recorded with a PCO Edge 4.2 sCMOS Camera at 10 s intervals. Data acquisition and analyses were accomplished using VisiView® 4.0.0.11 imaging software. Only GFP-positive cells were selected for Jurkat-CAR cells.

4.6.2 Ca^{2+}-response during immunological synapse formation

To investigate the immunological synapse (later we refer to it as CAR-synapse) between the Jurkat CAR and the Raji cells, the synapse was formed at a ratio of 1:1. We used the CMTPX cell tracker (ThermoFisher, C34552). 1×10^6 of Raji cells were centrifuged for 5 min 300×g then 1 µM of CMTPX was added in serum-free culture medium. Cells were incubated for 30 minutes

at 37 °C in the dark. Afterward, cells were washed 2 times and resuspended in phenol red-free medium RPMI 10% FBS. The labeled Raji cells were plated in the petri dish with the Jurkat CAR at a ratio of 1:1. The Ca^{2+}-response with FURA-2 was recorded as described above except that the images were recorded every 30 s for 1 hour without a change in the solutions or application of TG. The recording starting time point is at the moment of adding the Raji cells. The same experiment was also performed with crosslinking the Kv1.3 and with adding only a secondary antibody (IgG isotype) as described below. Only engaged cells were analyzed

Table 4: Recipe for the solutions of Ca^{2+} measurements

	2 mM Ca^{2+}	**0 mM Ca^{2+}**
NaCl (mM)	143.3	143.3
KCl (mM)	4.7	4.7
$MgCl_2$ (mM)	1	1
$CaCl_2$ (mM)	2	0
glucose (mM)	5.5	5.5
EGTA (mM)	0	0.1
HEPES (mM)	10	10
pH	7.35	7.35

4.6.3 Cytotoxic function validation of Jurkat-CARs

To evaluate the cytotoxic potential of Jurkat-CAR cells and to confirm the model, we conducted a Calcein Red-AM based cytotoxicity assay. Initially, Raji cells (the target cells) were stained with Calcein Red-AM. A total of 3×10^6 cells were centrifuged for 5 minutes at 300×g and subsequently resuspended in PBS. The cells were stained with 1 µM of dye for 30 minutes at 37 °C in the dark. Following this, the cells were plated into an 8-well Ibidi chamber containing phenol red-free RPMI supplemented with 1% FBS. In the co-culture setup, the ratio of target to effector cells (T: E) was maintained at 1:2. The cells were then incubated for 3 hours in a humidified cell culture incubator at 37 ° C. The recorded images were analyzed using Image J software with the ROI tool to assess the intensity of Calcein Red-AM.

4.6.4 Cytotoxic assay of CAR-T cells

To examine the specific cytotoxic effects of CAR-T cells, we employed a luciferase-based cytotoxicity assay. MDA, JIMT-1, and N87 cells that express eGFP/ffLUC were plated in 96-well flat bottom plates at a density of 3×10^4 cells per well in triplicate. After 24 hours, various effector cells were introduced at a 0.5:1 or 1:1 ratio of effector to tumor cells. The wells that did not contain effector cells acted as untreated controls. Following another 24 hours, luciferase activity was measured using a luciferase assay kit in accordance with the manufacturer's guidelines (Promega, Madison, WI, USA) and a Synergy HT luminometer (BioTek, Winooski, VE, USA).

4.7 CAR and Kv1.3 colocalization

Jurkat CAR cells were cultured on poly-L-lysine coverslips for 30 minutes at 37 °C (2×10^5 cells / coverslip) within a humidified chamber, followed by three washes with PBS at room temperature. The cells were then fixed using 1% formaldehyde for 10 minutes at room temperature. To prevent non-specific binding, 20% FBS in PBS was added to the cells for 30 minutes at room temperature. For the staining of Kv1.3, we employed the anti-Kv1.3 (KCNA3) extracellular antibody (Alomone Labs) Rabbit IgG at a dilution of 1:50 in 10% FBS-PBS, incubating overnight at 4 °C. Subsequently, the cells were washed with PBS, and the secondary antibody, Alexa 647 goat anti-rabbit, was applied at a dilution of 1:800 in PBS for 45 minutes on ice in the dark. The coverslips were washed three times with PBS and then mounted onto slides using Fluromount G. Images were captured using a Nikon N–STORM confocal microscope. To detect the signal, laser wavelengths of 488 and 647 nm were utilized based on the fluorescent intensity of GFP and Alexa Fluor 647. The recorded images were analyzed with Image J software utilizing the colocalization 2 plugin.

4.8 Immuno-staining for CAR-synapse

To explore the immunological synapse, which will be referred to as the CAR-synapse, between Jurkat-CAR and Raji cells, a 1:1 ratio was utilized to form the synapse. Initially, the cells were combined and co-centrifuged for one minute at 37 °C with 200×g. The resulting mixture was then placed onto coverslips that had been treated with poly-L-lysine and incubated for sixty minutes at 37° C. Subsequently, the cells were fixed using 4% formaldehyde for ten minutes, washed three times with PBS, and blocked with a solution of 20% FBS-PBS for forty-five

minutes. Following this, Kv1.3 channels were labeled as per the colocalization protocol, and the next day, the cells were permeabilized using 0.1% TritonX-100, with blocking conducted using 20% BSA-PBS for 45 minutes at room temperature. The cells were washed three times with PBS and labeled with the primary antibody CD19 (HIB19 from Biolegend) in 10% BSA-PBS, followed by incubation at 4° C overnight. Afterward, the cells were washed again three times with PBS, and an anti-mouse AlexaFluor-647 IgG was introduced (1:1000 dilution, for forty-five minutes at room temperature in the dark). Finally, the cells were washed with PBS, and the coverslips were mounted onto microscopy slides using Fluoromount-G. The samples were analyzed using a Nikon confocal microscope, with excitation lasers set to 488, 561, and 647 nm, and the images were processed using Image J software. To assess the accumulation ratio of Kv1.3, we employed the method previously described [180].

4.9 Ca^{2+} imaging in CAR synapse

The immune synapse was established between Raji and Jurkat CAR cells / Jurkat NT/ Jurkat-pBMN, to stain the target cells, we utilized the CMTPX cell tracker (ThermoFisher, C34552). A total of 1×10^6 Raji cells were centrifuged for 5 minutes at 300×g, after which 1µM of CMTPX was added to serum-free culture medium. The cells were incubated for 30 minutes at 37 °C in the absence of light. Subsequently, the cells were washed twice and resuspended in phenol red-free RPMI medium supplemented with 10% FBS. The labeled Raji cells were then plated in a petri dish alongside the Jurkat-CAR cells at a 1:1 ratio. The Ca^{2+}-response was recorded using FURA-2 as previously described, with the exception that images were captured every 30 seconds for one hour without switching the solutions or applying TG. The recording commenced at the moment the Raji cells were added. Additionally, the same experiment was conducted with crosslinking of Kv1.3 and the inclusion of only secondary antibody (IgG isotype) as detailed below. Only the synapse-engaged cells were subjected to analysis.

4.10 Kv1.3 crosslinking

Kv1.3 channels were immobilized using antibody complexes formed by rabbit anti-Kv1.3 antibody and anti-rabbit goat IgG. Initially, Jurkat-CAR cells were placed on ice for one hour and incubated with polyclonal anti-Kv1.3 antibody targeting an extracellular epitope at a ratio of 100:1 of antibody to Kv1.3 α subunit (0.8 µg antibody per 10 ml of cell suspension containing 2 million cells/ml). This concentration was established based on the average expression of approximately 400 Kv1.3 channels per cell, considering that each channel comprises four α

subunits. Following the incubation with Kv1.3 antibody, a subsequent 30-minute incubation with anti-rabbit IgG was conducted. Control cells underwent identical experimental procedures, with the addition of an isotype IgG, referred to as the Ab2 condition.

4.11 Statistical analysis

For our statistical analysis, we used the GraphPad Prism software version 8.0.1. One-way ANOVA or ANOVA on ranks tests were performed for the multiple comparison. For the two groups' comparison, we conducted unpaired t-test or Mann–Whitney test. The value of $p < 0.05$ was set as a significant difference. The results were shown as the mean ± standard error of the mean (SEM).

5 RESULTS

5.1 To unveil the functional role of Kv1.3 channel localization in Jurkat-CAR cells

5.1.1 Establishment of Jurkat-CARs anti-CD19

As the first step, our aim was to establish a 3rd generation CAR cell line targeting the CD19 molecule on the B-cell surface. The Jurkat T cell line generated stably expressing this CD19-CAR construct (Jurkat-CAR) via retroviral transduction was evaluated by fluorescence-activated cell sorting (FACS) for sGFP positivity, i.e. CAR presenting cells (Figure 12, 95 % of cells were sGFP^{+}). In order to evaluate the functionality of this model, we performed a Calcein Red-AM-based killing assay adopted from a study by Carsten Kummerow et al. [167]. Calcein Red-AM is a cell-permeant fluorescent probe. The cell vitality of the cells is proportional to the intensity of Calcein Red. The increase in the nonspecific membrane permeability of target cells, here we used CD19^{+} Raji B cell line as a target cell, leads to efflux of the dye which reports the irreversible phase of cell death. The results of the killing assay shown in Fig. 12B reveal that the intensity of Calcein Red dropped when Raji cells were co-cultured for 3 hours with Jurkat-CARs, unlike for non-transduced Jurkat cells (NT-Jurkat): this concludes that Jurkat-CARs specifically eliminates the target cells even within this short period. Therefore, the generated CAR-expressing model cell line could be applied in the subsequent experiments related to the ion channel, specifically Kv1.3.

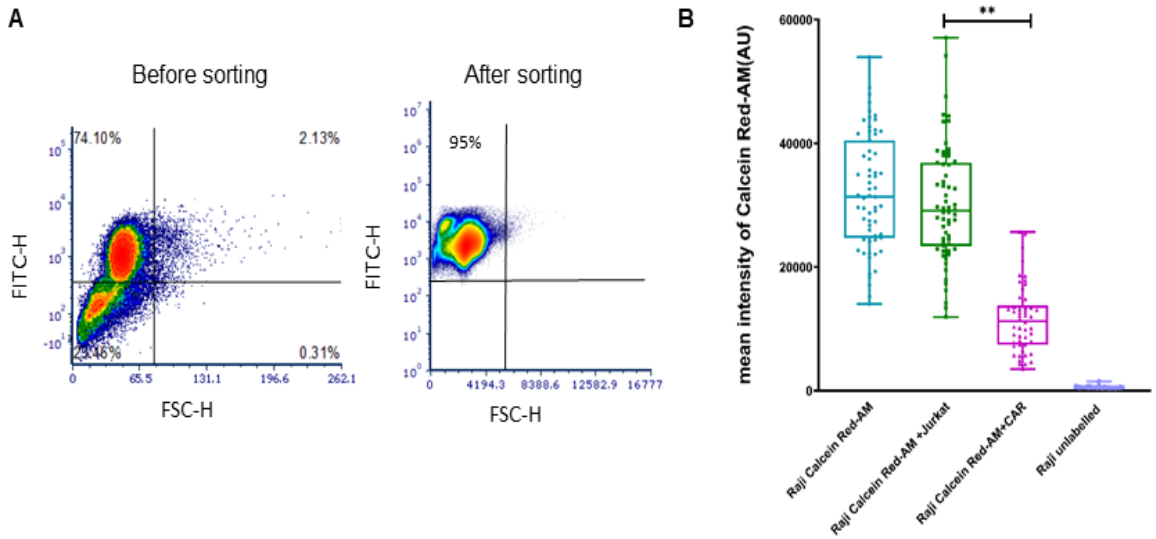

Figure 12**: Generation and validation of CAR T cell line. (A) (left)** sGFP-FSC density plot of the CD19-CAR transduced Jurkat cells. Here 74% of cells were sGFP positive. sGFP was detected in the FITC channel. (**right)** The dotplot (FSC vs. sGFP) of sorted Jurkat-CARs, cells showed 95 % positive GFP cells. **(B)** Calcein Red-AM-based killing assay for Jurkat-CARs and NT-Jurkats. Boxplot of Calcein Red intensity values, each symbol represents the mean intensity of Calcein Red for a cell. Raji Calcein Red-AM: Raji B cells loaded with dye, no effector cells added; Raji Calcein Red-AM + Jurkat: dye loaded Raji cells incubated with NT-Jurkats; Raji Calcein Red-AM + CAR: dye loaded Raji cells incubated with Jurkat-CARs, Raji unlabeled: unstained Raji cells. The E:T ratio is 1:1, measurements were performed on three different days, N ≥ 30, **: p<0.01.

5.1.2 Biophysical characterization of Kv1.3 channel of Jurkat-CARs

After the validation of the Jurkat-CAR cell line, we attempt to investigate the effect of the introduction of CAR into the Jurkat T cell line on the kinetics of the voltage-gated potassium channel Kv1.3, which contributes to the Ca^{2+}-activated pathway in T cells. Current of Kv1.3 channels in Jurkat-CARs, NT-Jurkats and Jurkat-PBMNs (empty pBMN vector transduced cells, transduction control) were analysed to determine the biophysical parameters of the channel. As it is illustrated in *Figure 13* A and B, the activation and inactivation kinetics were the same in Jurkat-CARs compared to NT-Jurkats and Jurkat-PBMNs (τ_a for NT-Jurkat is 0.65 ± 0.04 ms, τ_a for Jurkat-PBMN is 0.64±0.04 ms,τ_a for Jurkat-CAR is 0.85 ±0.08 ms), (τ_i: NT-Jurkat: 201.3 ± 21 ms, Jurkat-PBMN: 168.2 ± 11.4 ms, Jurkat-CAR: 220.4 ± 20m,). Next, we also evaluated the equilibrium parameters of membrane potential dependence of activation: the test-potential vs. normalized conductance curves show that the slope factor (k) is the same for Jurkat-CARs/NT-Jurkats and Jurkat-CARs/ PBMN-Jurkats (slope: NT-Jurkat: 9.84 ±0.6 mV, Jurkat-CAR: 10.95 ±0.6 mV, Jurkat-PBMN: 13.80 ± 1mV, $p > 0.05$, Fig 13C). The half-

maximal voltage ($V_{1/2}$) was higher for the Jurkat-CARs than NT-Jurkats (V_{half} for NT-Jurkat: -29.24 ±3.2 mV, Jurkat-CAR: -20.37 ± 1.9mV) as indicated by the rightward shift of the steady-state activation curve. The comparison of the half-maximal voltage between NT-Jurkats/Jurkat-PBMNs and Jurkat-CAR/Jurkat-PBMN was non-significant (V_{half} for Jurkat-PBMN: -23.43 ± 1 mV, $p>0.05$). These results show that the Kv1.3 steady-state activation is slightly affected by the presence of the CAR receptor on the membrane and could be as well partially attributed to the viral transduction itself. Driven by these discoveries, we subsequently conducted a Ca^{2+}-imaging to gain an understanding of this pathway.

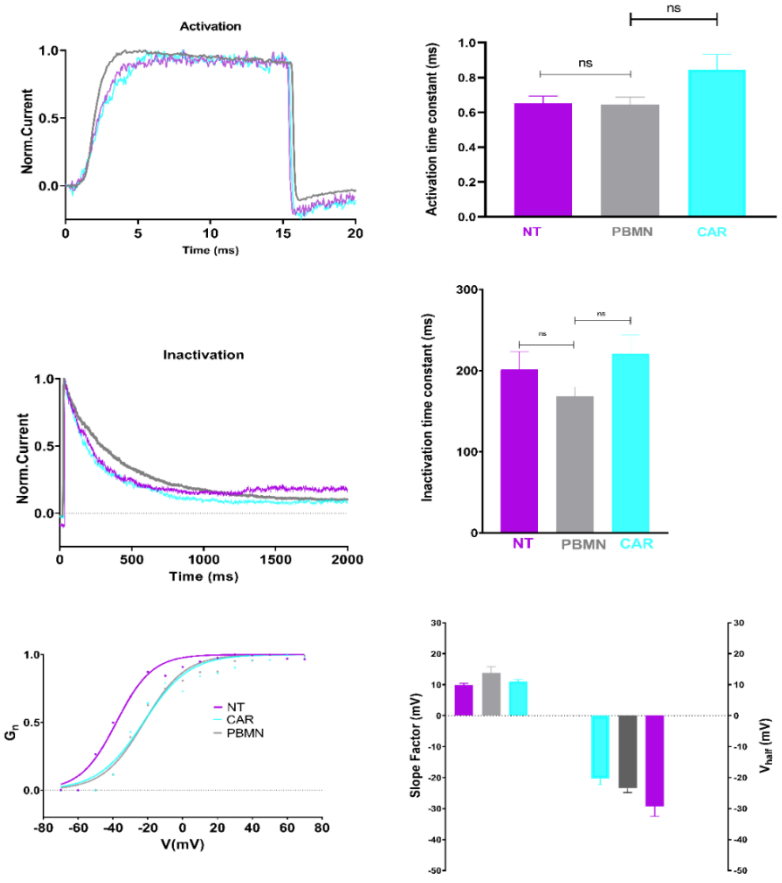

Figure 13: **Biophysical properties of Kv1.3 channel in Jurkat-CARs. (A) Activation kinetics left**: Normalized current traces of an NT-Jurkat, Jurkat-CAR, Jurkat-PBMN cell recorded upon 15-ms-long, +50mV depolarization, holding was -120 mV. **Right:** Kv1.3 current activation time constant of Jurkat-CAR, NT-Jurkat and Jurkat-PBMN cells. **(B) Inactivation kinetics, left:** current traces recorded upon depolarization to + 40mV for 2 s from – 120 mV holding potential. Right: inactivation time constant for Kv1.3 current in Jurkat-CAR, NT-Jurkat and Jurkat-PBMN cells. **(C) Voltage–dependence of steady-state activation, left:** the test-potential vs. normalized conductance along with the best-fit Boltzmann curves for a Jurkat-CAR, NT-Jurkat and Jurkat-PBMN cell, **Right**: the equilibrium parameters activation, $V_{½}$, and the slope factor (k), N = 3-8, ns: not significant.

5.1.3 Jurkat-CARs has a lowered TG-induced Ca^{2+}- response

To assess the functional expression of CRAC channels, we conducted FURA-2 based Ca^{2+}-imaging experiments. Following stimulation with thapsigargin (TG) and the reintroduction of 2 mM extracellular Ca^{2+} in the presence of TG, an increase in cytosolic Ca^{2+} was observed, attributed to the influx of Ca^{2+} through the pore created by CRAC channels. The control NT-Jurkat and Jurkat-PBMN cells had a typical Ca^{2+}-response as shown in *Figure 14* A, while the representative trace of the cytosolic Ca^{2+} level (average of 20-30 cells) shows that Jurkat-CARs had a significantly lower CRAC-related response, i.e. the SOCE is lowered. The ratio of intensity ratios detected in the presence of 2 mM Ca^{2+} over the baseline (0 mM Ca^{2+} solution with TG, just before addition of 2 mM Ca^{2+}) was significantly higher in NT-Jurkat compared to Jurkat-CARs (*Figure 14* B, p = 0.009) and significantly different between Jurkat-PBMN and Jurkat-CAR (p=0.01). These findings report that the effect observed on the Ca^{2+} response is linked to the CAR expression and not because of the retroviral transduction.

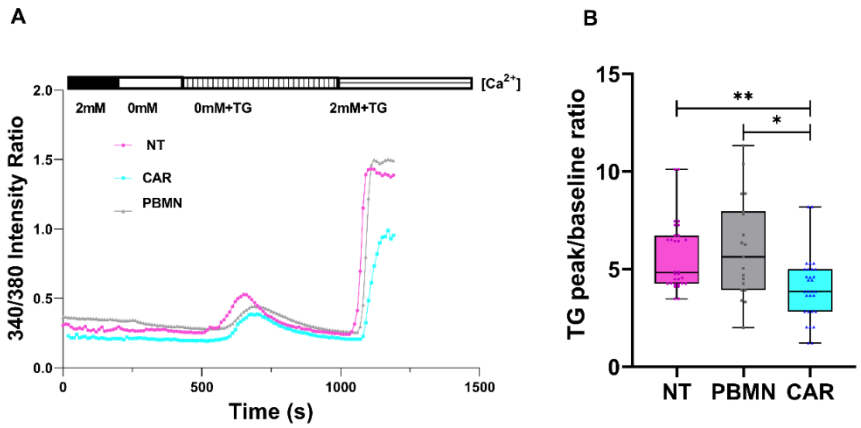

Figure 14: **Cytosolic Ca^{2+} measurements using FURA-2 in Jurkat-CAR, NT-Jurkat and Jurkat-PBMN cells**. **(A)** Cytosolic Ca^{2+} representative traces of Jurkat-CAR (blue), Jurkat-NT (pink) and Jurkat-PBMN (gray) on the 340nm/380nm intensity ratio. For the representative traces, at least 30 cells were recorded. **(B):** Boxplot of baseline Ca^{2+} intensity ratios for Jurkat-CAR (CAR, blue), Jurkat-NT (NT, pink) and Jurkat-PBMN cells (PBMN, gray). Each point represents a single-cell value, N=20-30, *: $p < 0.05$.

5.1.4 Kv1.3 channel is co-localized with the CAR receptor and present in the IS

The immune synapse (IS) represents a dynamic interaction between the target cell and the effector cell. Prior research has indicated that Kv1.3 channels relocate into the IS, suggesting the potential to modulate the activity of this channel to influence the signaling initiated within the IS [168]. Consequently, we investigated the localization of CARs and Kv1.3 channels in

Figure 15 Confocal images of Jurkat-CAR cells labeled with Kv1.3 antibody are presented in *Figure 15*A, where the patchy fluorescence of Kv1.3 channels and the sGFP signal of CAR exhibit significant overlapping regions. Utilizing Image J software, we evaluated the co-localization of Kv1.3 and CAR, finding that the Pearson correlation coefficient (mean R-value was 0.54) indicates the proximity of these two proteins within the cell membrane. No previous studies have reported the presence of the Kv1.3 channel in the immunological synapse formed between a CAR T cell and a target Raji B cell (here referred to as the CAR synapse or CS to distinguish it from the CD3/MHC related immune synapse). Therefore, we established a CAR synapse between Jurkat-CAR cells and Raji cells, evaluating the rearrangement of Kv1.3 channels within the contact region between the effector and target cells (*Figure 15* C). To verify the formation of the CS, we monitored the accumulation of CAR in the contact area of the two cells [169]. *Figure 15* C illustrates that Kv1.3 from Jurkat-CARs redistributes to the CS, further corroborated by the accumulation ratio (AR) value of 2.99 ± 0.6 ($p = 0.001$) displayed in *Figure 15*D. The significance of Kv1.3 in synaptic regions has been previously described: it modifies the Ca^{2+}-dependent signaling pathway and may lead to T cell hyperactivity [170].

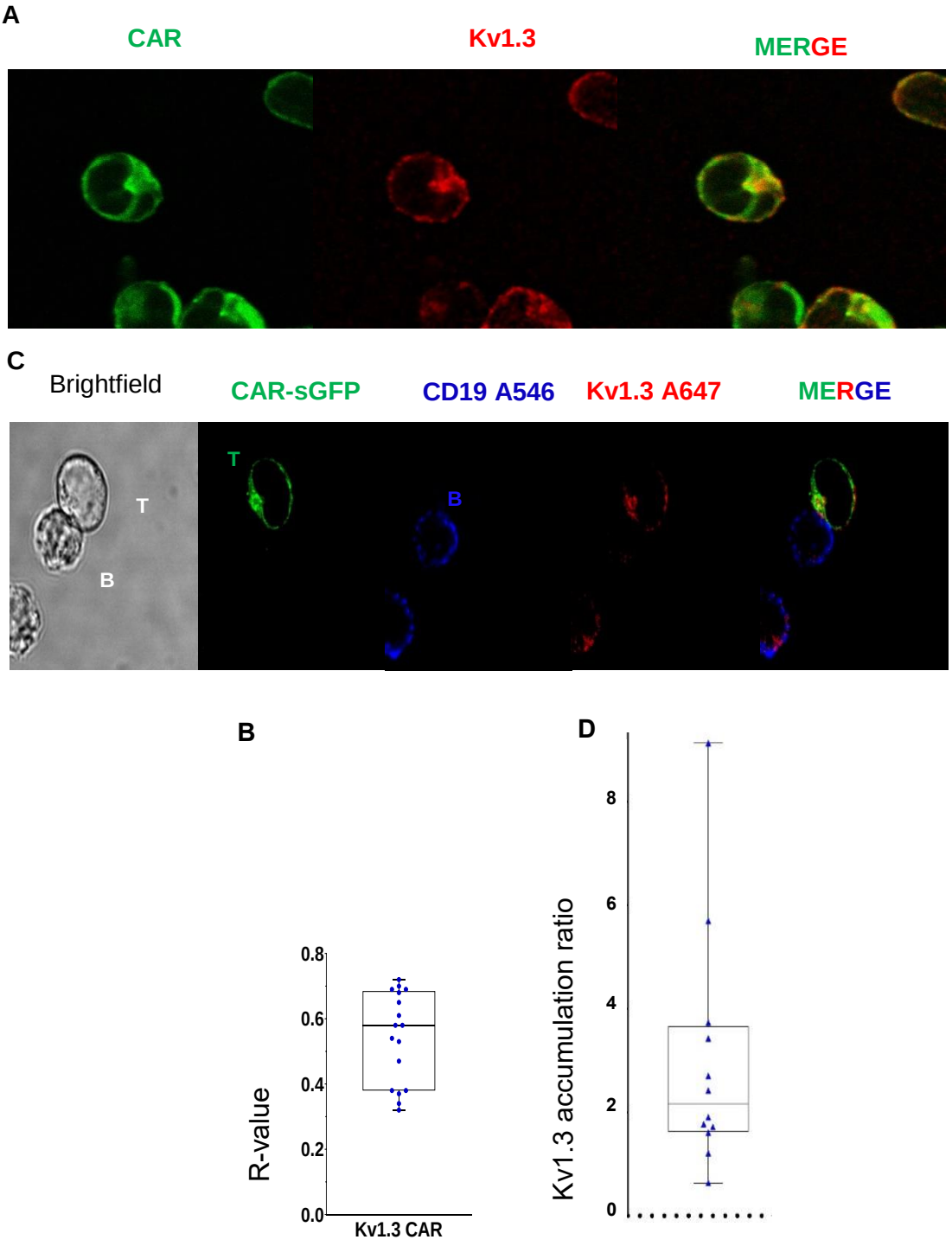

Figure 15: **Colocalization of CAR and Kv1.3 in Jurkat-CARs and Kv1.3 accumulation in the immunological synapse between Jurkat-CAR and Raji. (A)** Confocal images of Jurkat-CAR cells stained with anti-Kv1.3 antibody (2nd ab is goat anti-rabbit IgG with Alexa-647), left: CAR with sGFP (green), mid: Kv1.3 with Alexa 647 (red), right: merge of green and red channels. **(B)** Dot-plot of Pearson coefficients for colocalization of CAR and Kv1.3, N =17. **(C)** Confocal images of immune synapse formed between a CAR (green) cell and a Raji (blue) cell. Kv1.3 was stained with rabbit anti- Kv1.3 and goat anti-rabbit Alexa647, Raji cells stained with mouse anti-CD19 and goat anti-mouse Alexa546, the merge of the channels (blue and red) shows the accumulation of Kv1.3 in the CAR synapse, **(D)** Boxplot of Kv1.3 accumulation ratio observed in the synapse after 60 minutes.

5.1.5 The inhibition of the Kv1.3 recruitment to the synapse abolishes target cell elimination of Jurkat-CAR cells

The role of Kv1.3 in the CAR-synapse formed between Jurkat-CARs and Raji cells is still unclear. In this study, we aimed to investigate whether the inhibition of Kv1.3 channels' relocation to the synapse affects the canonical function of CAR cells, specifically their ability to eliminate target cells. As in prior experiments, we assessed the killing capacity of Jurkat-CARs by obstructing the accumulation of Kv1.3 channels at the contact site through antibody cross-linking, as previously outlined [183], and subsequently co-incubated these modified cells with Raji target cells. The results shown in *Figure 16* illustrate that the immobilization of Kv1.3 channels diminished the target cell elimination capability of Jurkat-CARs unlike the effect with cells treated solely with the secondary antibody. These results indicate that the disruption of Kv1.3 channels' membrane redistribution to the contact site in Jurkat-CARs significantly impacts their target elimination efficiency.

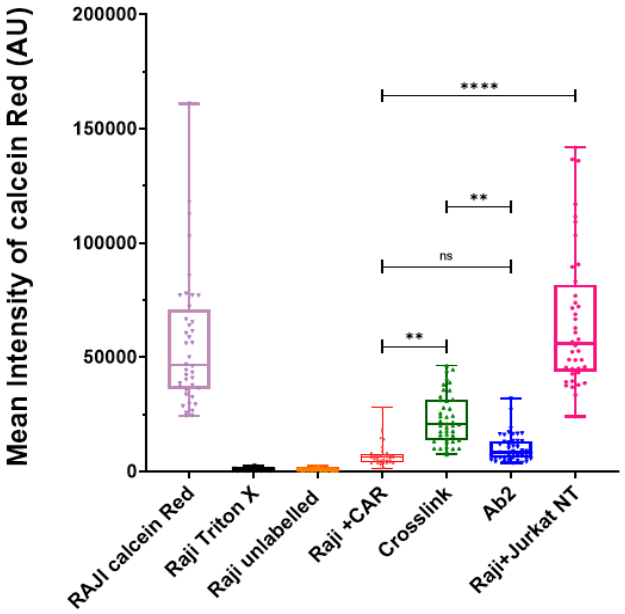

Figure 16: **Kv1.3 immobilization suppresses target cell elimination.** Boxplot of Calcein Red intensity values, each symbol represents the mean intensity of Calcein Red for a cell. Raji Calcein Red-AM: Raji B cells loaded with dye, no effector cells added; Raji +Triton X; Raji Calcein Red-AM + Jurkat cells; Raji cells incubated with NT-Jurkats; Raji Calcein Red-AM + CAR: dye loaded Raji cells incubated with Jurkat-CARs, Raji unlabeled: unstained Raji cells ;Raji Calcein Red-AM + CAR with crosslinking Kv1.3; Raji Calcein Red-AM + CAR with secondary antibody only. Kv1.3 channels were cross-linked using a ratio of 100: 1 of antibody Kv1.3 α subunit, the E: T ratio is 1:2, and measurements were performed on three different days, **: $p<0.01$.

5.1.6 Kv1.3 location affects the Ca^{2+}response of Jurkat-CARs

It has been previously reported that the redistribution and accumulation of the Kv1.3 channel within the immune synapse plays a role in shaping Ca^{2+}-signaling [170]. Additional studies have indicated that the residency of ion channels (Orai1/CRAC and Kv1.3) at the immune synapse affects the Ca^{2+}-response of T cells [171, 172]. Therefore, we conducted Ca^{2+}-imaging measurements while forming a CAR-synapse between a Jurkat-CAR and a Raji cell to explore the impact of inhibiting the trafficking of Kv1.3 into the synapse. These experiments were structured to assess the Ca^{2+}-response of NT-Jurkat cells, Jurkat-CARs, Jurkat-CARs with cross-linked Kv1.3, and Jurkat-CARs in the presence of the isotype IgG (secondary antibody), referred to as the Ab2 condition. Upon interacting with the target cell, all NT-Jurkat cells exhibited, as anticipated, no alteration in the baseline Ca^{2+}-level, which remained constant throughout the entire recording duration (60 min, *Figure 17* D). In contrast, Jurkat-CARs demonstrated a diverse response in Ca^{2+}-level upon contact with a Raji cell: 1) the majority (47%) of cells exhibited an oscillatory response until the conclusion of the recording period (*Figure 17* A), 2) a smaller proportion of cells (30%) displayed oscillatory Ca^{2+} levels with a decreasing baseline *Figure 17* B), and 3) a minority (23%) showed isolated Ca^{2+}-spikes without oscillation (*Figure 17* C, *Figure 17* E). In the case of Jurkat-CARs in the presence of Ab2, the calcium response was comparable to that observed in its absence (*Figure 17* E). Similar to NT-Jurkat cells, the Kv1.3 trafficking-restricted Jurkat-CAR cells (where Kv1.3 was cross-linked prior to Fura-2 loading) did not exhibit any change in the intracellular Ca^{2+}-level upon interaction with a Raji cell (*Figure 17* D). The variations observed in Ca^{2+}-signaling may be attributed to differences in downstream signaling pathways, underscoring the significance of Kv1.3 relocation in the initiation of target cell killing mechanisms.

This may be from the differences in immunoreceptor tyrosine-based activation motifs (ITAMs) between the TCR and CAR that initiate the phosphorylation cascade.

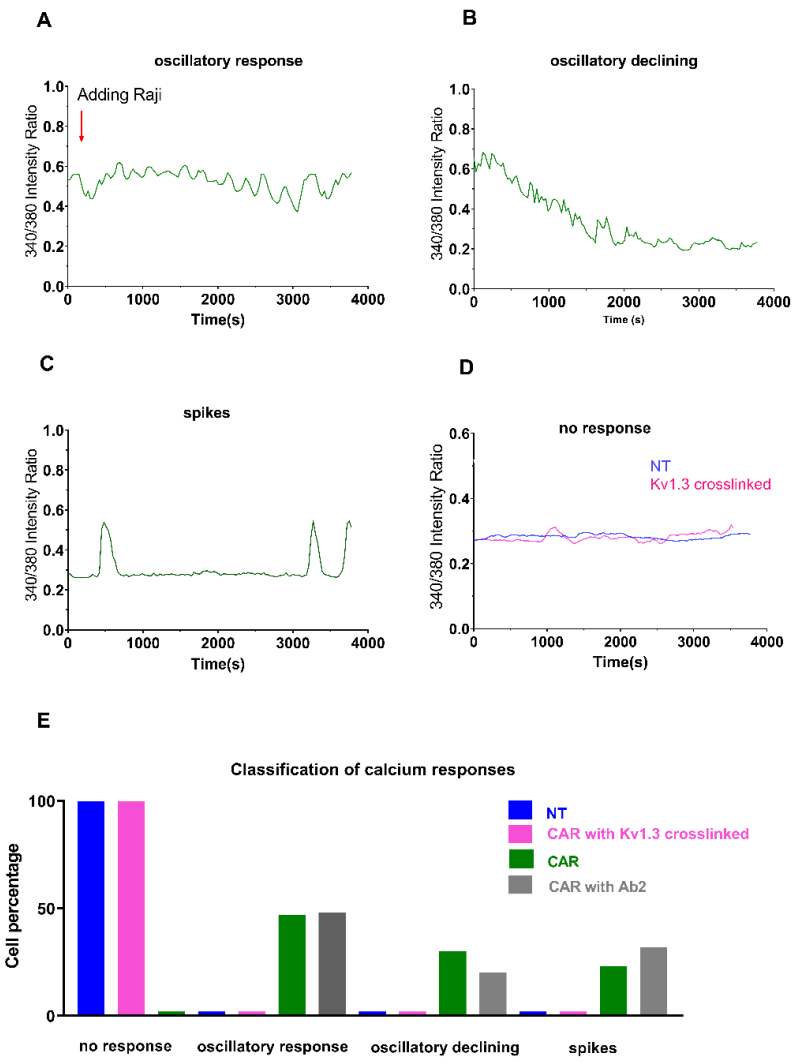

Figure 17: **Ca^{2+}-response of Jurkat-CARs diminishes in the lack of Kv1.3 CS-accumulation. (A)** Representative traces of cytosolic FURA-2-based Ca^{2+} measurements in Jurkat-CARs: oscillatory response with steady baseline, **(B)**: oscillatory with declining baseline, **(C)**: multiple, lone spikes**. (D)** Response of NT-Jurkat and Jurkat-CAR cells upon crosslinking Kv1.3 in a synapse with a Raji CD19 cell. The arrow indicates the addition of Raji target cells, **(E)** Classification of Ca^{2+}-response in NT-Jurkats, Jurkat-CARs, Kv1.3-crosslinked Jurkat-CARs and Jurkat-CARs incubated with 2nd antibody only (Ab2). N≥30.

5.2 Determine the expression and role of K^+ channels in anti-HER2 3rd generation CAR-T cells

5.2.1 Kv1.3 and KCa3.1 expression of CAR T cells

The incorporation of the CAR construct into T cells can influence the expression of ion channels in the cell membrane. This alteration can significantly impact the Ca^{2+}-dependent cellular processes within T cells. Motivated by the previous results in CAR-Jurkat model, we initially examined whether the levels of the ion channels KCa3.1 and Kv1.3 in CAR T cells were affected by the transduction of the specific CAR protein. Utilizing the patch-clamp technique, we assessed the expression levels of these two channels in third-generation CAR-T cells compared to control cells (non-transduced or NT T cells). We implemented the ramp protocol (with 1 µM free Ca^{2+} in the pipette solution) to simultaneously record the currents of the KCa3.1 and Kv1.3 channels, as illustrated in *Figure 18* A. The KCa3.1 level is indicated by

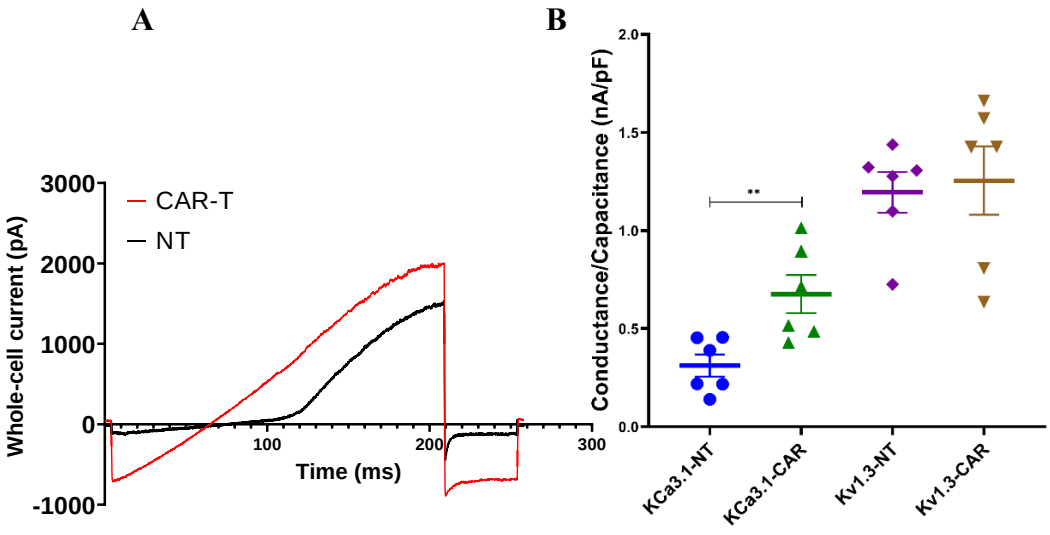

Figure 18: **Kv1.3 and KCa3.1 level of CAR T cells.** (**A**) Whole-cell current recorded in non-transduced (NT) T cell (black line) and a 3rd generation CAR-T cell (red line) using 200 ms long voltage-ramp protocol ranging from –120 mV up to +50 mV; holding potential was −70 mV. Note the steeper slope of the linear part of the trace for 3rd-generation CAR T cell (higher KCa3.1 conductance expression compared to the NT control). (**B**) Scatter plot of Kv1.3 and KCa3.1 capacitance-normalized conductance of the 3rd-generation CAR transduced and NT cells (thick horizontal line: mean, error bars: SEM, $n \geq 6$ (donor number), $N \geq 5$ (number of cells/ donor), and **: $p < 0.01$.

The slope of the curve, where the Kv1.3 channels remain inactive (more negative than −40 mV), while the peak current of +50 mV, observed at the end of the ramp after subtracting the KCa3.1 current, reflects the magnitude of the Kv1.3 current. Through this protocol, we

estimated the expression levels of these two channels in both control/non-transduced (NT) and CAR T cells: *Figure 18* B demonstrates that the KCa3.1 whole-cell, capacitance-normalized conductance level was elevated in the third-generation CAR T cells compared to the NT T cells (0.31 nS/pF for NT versus 0.64 nS/pF for CAR T cells; $p = 0.009$). Conversely, the Kv1.3 level did not exhibit any significant difference when compared to the NT cells (1.19 nS/pF for NT versus 1.25 nS/pF for CAR T cells; $p = 0.77$).

5.2.2 $CD4^+$ and $CD8^+$ CAR T cells have difference in Kv1.3 and KCa3.1 expression

The third-generation CAR T cells exhibited a significantly higher expression of KCa3.1 in comparison to the control group, while the expression levels of Kv1.3 remained unchanged. Subsequently, we aimed to determine whether there was a variation in the expression of the ion channels, KCa3.1 and Kv1.3, between the $CD4^+$ and $CD8^+$ CAR T cells, given that the cytotoxic efficiency differs between these two populations. Therefore, we assessed the conductance of KCa3.1 and Kv1.3 in these subsets of T cells. We utilized the same protocol as previously described, with the exception that we employed the antibody adhesion technique to isolate the $CD4^+$ or $CD8^+$ subpopulations. Our findings indicated that the $CD8^+$ CAR T cells demonstrated a higher level of KCa3.1 expression when compared to the CD8 NTs (0.42 nS/pF for $CD8^+$ NT and 0.895 nS/pF for $CD8^+$ CAR T cells; $p = 0.04$); however, no significant differences were observed in the KCa3.1-normalized conductance of the $CD4^+$ cells or in the Kv1.3 expression across all groups as illustrated in Figure 19.

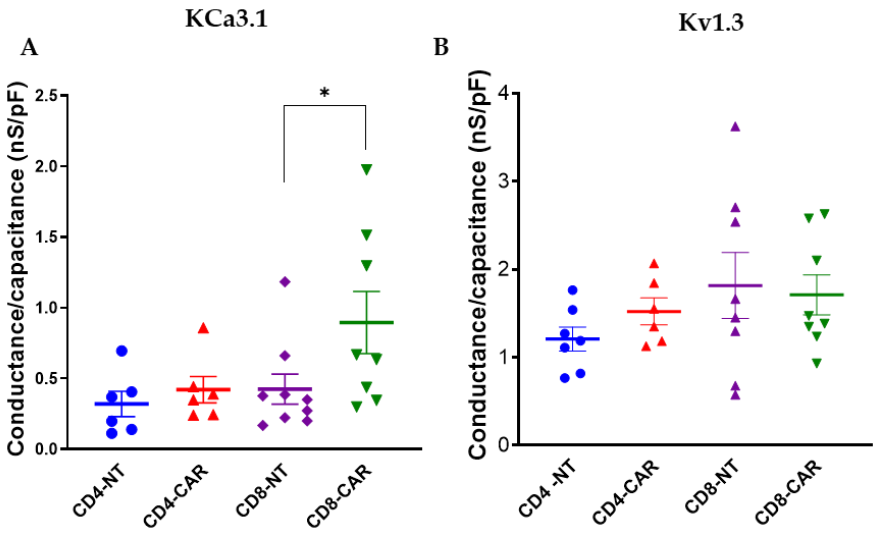

Figure 19: **KCa3.1 channel capacitance-normalized conductance is higher in CD8$^+$ 3rd-generation CAR T cells**. (**A**) KCa3.1 conductance normalized to capacitance in CD4 and CD8 NT and 3rd generation CAR T cells. (**B**) Kv1.3 capacitance-normalized conductance of NT and 3rd generation CD4 and CD8 CAR T cells. Thick horizontal line: mean, error bars: SEM, each symbol: mean value for a donor, n ≥ 5 (number of donors), N ≥ 5 (number of cells per donor), and *: $p < 0.05$.

5.2.3 CD8$^+$ CAR T cells Ca^{2+} response is suppressed

As previously mentioned, the KCa3.1 and Kv1.3 channels are responsible for maintaining the negative membrane potential, which is crucial for facilitating the influx of Ca^{2+} through CRAC channels. The activation of CRAC initiates various pathways that are integral to the effector functions of T cells. Consequently, the Ca^{2+} response induced by thapsigargin (TG) in third-generation CD4$^+$/CD8$^+$ CAR and NT T cells was evaluated by measuring the changes in cytosolic Ca^{2+} using FURA-2 radiometric imaging. *Figure 20* A illustrates the time course of the Ca^{2+} measurements. The averaged traces presented in *Figure 20* A indicate that all T cell types exhibit a similar baseline Ca^{2+} level, contrasting with the Ca^{2+}-response observed during CRAC activation and the subsequent reintroduction of extracellular Ca^{2+}. Our findings reveal that the Ca^{2+}-responses of NT CD8$^+$, NT CD4$^+$, and third-generation CD4$^+$ CAR cells are comparable, whereas the CD8$^+$ CAR cells displayed a significantly diminished response in comparison to the control cells. The 2 Ca^{2+}/0 Ca^{2+} ratio (peak over baseline) depicted in Figure 20B, which reflects CRAC expression in the cells, was significantly lower in the third-generation CD8$^+$ cells relative to the CD8$^+$ NT control ($p = 0.02$).

These findings may imply that the Ca^{2+} influx through the CRAC channel is influenced by the presence of the CAR in the membrane, potentially affecting their cytotoxic capabilities.

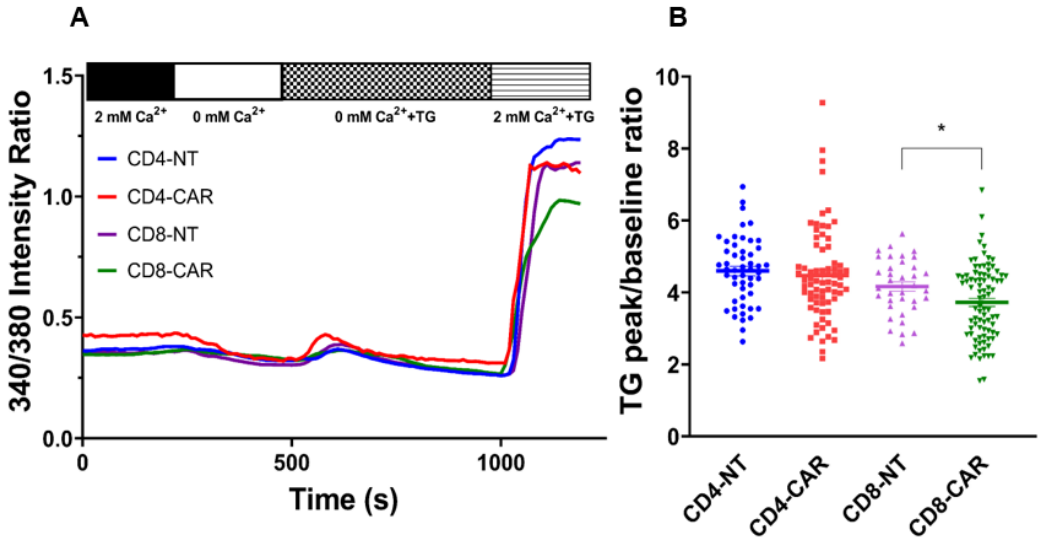

Figure 20. **Cytosolic Ca^{2+}-response of $CD4^+$ and $CD8^+$ 3rd-generation CAR T cells.** (**A**) The representative traces are the average of 18 $CD4^+$ NT T cells (blue), 20 $CD4^+$ CAR T cells (red), 12 $CD8^+$ NT cells (purple) and 14 $CD8^+$ CAR T cells (green). (**B**) Scatter plot of Ca-fold change (ratio measured after addition of 2 mM Ca^{2+} over before addition of 2 mM Ca^{2+} in the presence of TG) in 3rd-generation CAR and NT, $CD4^+$ and $CD8^+$ cells; each point represents a cell. *: $p < 0.05$.

5.2.4 The suppression of Kv1.3 and KCa3.1 facilitate the killing potential of $CD8^+$ CAR T cells

$CD8^+$ cytotoxic cells are likely to play a crucial role in the eradication of tumor cells, with K^+ ion channels contributing to the modulation of Ca^{2+} signaling [173]. Subsequently, we examined the cytotoxic activity of HER2-specific $CD8^+$ CAR T cells following the administration of Vm24 (a specific Kv1.3 blocker at 1 nM) and TRAM-34 (a KCa3.1 antagonist at 1 µM) in a firefly luciferase (ffLuc) activity-based cytotoxicity assay, utilizing a 1:1 effector to target (E:T) ratio with ffLuc-modified MDA-HER2, JIMT 1, and N87 target cells. MDA cells lacking HER2 expression were utilized as HER2-negative controls. Our findings indicate that CAR T cell populations effectively recognized and eliminated $HER2^+$ target cells (Figure 21B), whereas NT T cells exhibited no cytolytic activity, thereby confirming their specificity (Figure 21 A). The addition of the Kv1.3 inhibitor Vm24 significantly enhanced the target cell killing capacity of the $CD8^+$ CAR T cells, irrespective of the target cell type (MDA-HER: approximately 51%, JIMT-1: approximately 36%, and N87: approximately 55% reduction in luciferin intensity; Figure 21B ($p = 0.0004$) and Figure 21 A). Furthermore, the addition of

TRAM-34 (the KCa3.1 blocker) also augmented the killing efficacy of the CAR T cells *in vitro* against the HER2^{+} monolayer target cell cultures for each cell line evaluated (MDA-HER2: approximately 65%, JIMT-1: approximately 53%,and N87: approximately 46% decrease in luciferin intensity, Figure 21 B ($p = 0.0002$) and Figure 21 A.

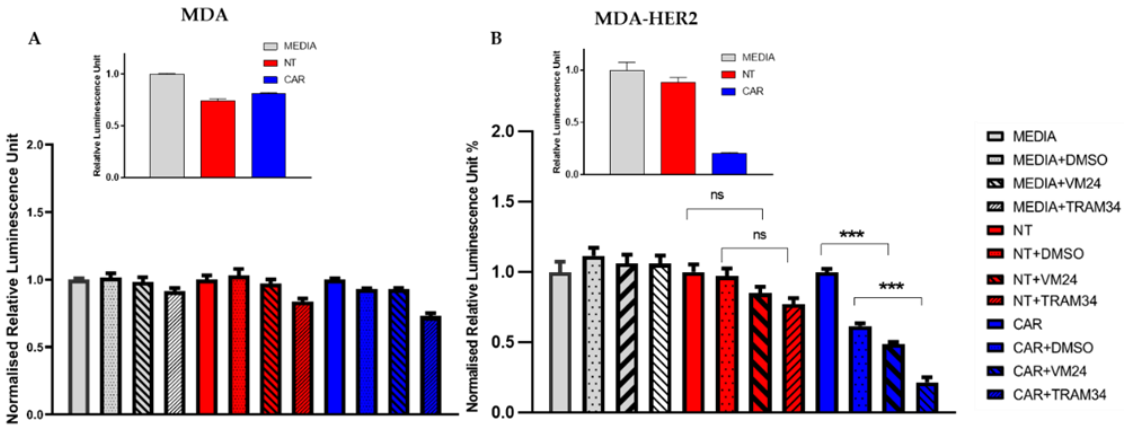

Figure 21**: KCa3.1 and Kv1.3 suppression enhances target cell elimination of CAR T cells**. Firefly luciferase-based cytotoxicity assay using HER2-speficic CAR T cells, (**A**) MDA (HER2 negative) and (**B**) MDA-HER2 (HER2^{+}), as targets at 1:1 ratio (E: T) (n = 4); the assay was performed in triplicates. Vm24 was applied at 1 nM, and TRAM-34 concentration was 1 µM. The intensity values in each group (gray (MEDIA) only target cells (MDA (left), MDA-HER2 (right)) were plated; red (NT): target cells with CD8^{+} NT cells were co-cultured; and blue (CAR): target cells and CD8^{+} CAR T cells were plated) were normalized to the first column of the group (grey to the MEDIA, red to the NT, and blue to the CAR) to emphasize the relative change within the group. Insert figures in both panels show the media-normalized luciferase intensities to visualize the killing capacity of CAR T cells. ***: $p < 0.001$; ns: not significant.

6 DISCUSSION

6.1 To unveil the functional role of Kv1.3 channel localization in Jurkat-CAR cells

In this part of the thesis, we sought to determine the role of Kv1.3 channel in Jurkat-CAR, which was reported previously as an adequate approach for characterization of CAR in T cells [174]. By employing the whole-cell patch-clamp technique, we revealed the biophysical characteristics of the Kv1.3 channel in Jurkat-CAR model. Our findings indicate a slight shift in the steady-state activation curve towards depolarizing potentials (rightward) in Jurkat-CARs, which is likely to influence Ca^{2+}-signaling. Driven by this observation, we assessed the Ca^{2+}-response of Jurkat-CARs: the CRAC-dependent Ca^{2+}-amplitudes were reduced when compared to NT-Jurkat and Jurkat-PBMN cells (Fig.14A). We hypothesize that the introduction of CAR may alter the expression of proteins that regulate thapsigargin-induced Ca^{2+}-uptake. Alternatively, the alteration in Kv1.3 activation could result in a decreased Ca^{2+}-level. Nevertheless, the optimal intracellular Ca^{2+}-level may vary for different functions, suggesting that this reduction could enhance the cytotoxic potential of Jurkat-CARs.

Furthermore, we demonstrated the co-localization of Kv1.3 with the CAR receptor, indicating a functional relationship between the CAR and the channel. On the other hand, we showed the accumulation of CARs alongside Kv1.3 channels at the synapse between Jurkat-CAR and Raji cells. Previous reports have indicated that the localization and persistence of Kv1.3 channels in T cells at the immunological synapse modulate the Ca^{2+}-response, which may contribute to T cell hyperactivity [175]. The co-localization of Kv1.3 with CD3 has been reported in T cells, suggesting that their proximity could have functional significance, as proposed in earlier research [176]. However, it is important to note that CD3 and exogenous Kv1.3 reside in different regions of the immunological synapse in CD4 cells. To investigate how the redistribution of Kv1.3 at the synapse affects effector functions, we inhibited Kv1.3 channel IS-trafficking in Jurkat-CARs as previously described [170].

The crosslinking experiment clearly demonstrated that the recruitment of the Kv1.3 channel is crucial for the effective performance of Jurkat-CARs: inhibiting Kv1.3 synapse redistribution partially diminished the killing capacity. We believe this can be explained by the followings: i) not all Jurkat cells express Kv1.3, allowing these cells to still induce cell death in target cells, ii) since Kv1.3 and CAR are likely located within the same membrane domain, the immobilization of Kv1.3 disrupts CAR's relocation to the synaptic area, resulting in no formation of encounters with target cells, iii) the Ca^{2+}-dependent pathway is not the sole mechanism for target cell elimination. The first point can be dismissed, as patch-clamp studies revealed the presence of Kv1.3 current in nearly every Jurkat-CAR cell. The second point is

also unlikely, given that the number of CARs significantly surpasses the number of Kv1.3 channels in Jurkat-CAR cells (figure 15). We believe there is enough CARs that can migrate to the synapse and trigger cell death in target cells. It is possible that the activation independent of Kv1.3 and Ca^{2+}-influx through CD28 and 4-1BB could explain this nuanced situation.

To reveal how the crosslinking of Kv1.3 channels influences the Ca^{2+}-dependent pathway, we examined the Ca^{2+}-response in Jurkat-CAR cells. When NT-Jurkat cells got in contact with Raji-target cells, no Ca^{2+} signal was detected over an extended duration (up to 60 minutes), clearly showing the specificity of the CAR-CD19 interaction. In contrast, the Ca^{2+}-signaling in Jurkat-CARs (and Jurkat-CARs treated solely with the secondary antibody, Ab2 condition, Fig. 17E) exhibited significant differences: the Ca^{2+}-levels showed periodic/oscillatory fluctuations that persisted until the 60^{th} minute. Previously, we indicated that the Ca^{2+}-response in Jurkat cells could be characterized by a single-peak response, with a few oscillations occurring over a brief period when these cells were stimulated via the CD3/TCR complex [171]. A distinction in Ca^{2+} signaling induced by TCR and CAR has been noted before; however, the flow cytometric analysis conducted here does not permit a suitable comparison [177].The crosslinking of Kv1.3 entirely eliminated the changes in Ca^{2+} levels during the formation of the Jurkat-CAR - Raji encounter. Nicolaou et al. previously reported that Ca^{2+}-signaling is also influenced by the localization of Kv1.3 at the immunological synapse, although their experiments involved T cells being activated through the CD3/CD28 pathway [172]. Therefore, we can conclude that modulating Kv1.3 could serve as a potential target for achieving improved therapeutic outcomes. It is important to mention that Jurkat cell line do not express the KCa3.1 channel, which contributes as well to the Ca^{2+} activated pathway [178]. Via this model, we wanted to examine the role of the Kv1.3 channel alone. The next step would be to study the role of ion channels in primary T cells.

6.2 Determine the expression and role of K^+ channels in anti-HER2 3^{rd} generation CAR-T cells

CAR T cell immunotherapy has emerged as a significant advancement in recent years. Despite impressive clinical successes, the ideal engineering of CAR cell constructs remains unresolved. Patients undergoing this treatment may experience life-threatening toxicities, and the limited effectiveness against solid tumors presents a challenge to address [179]. Ion channels in T cells, such as Kv1.3, KCa3.1, and CRAC, have been identified as crucial in regulating various cellular functions. The inhibition or knockdown of these channels impairs the proliferation and effector

functions of T cells [180]. However, there is still limited understanding of how these ion channels contribute to anti-tumor immunity in eliminating cancer cells, particularly in CAR T cells.

In this part of the study, we examined the functional expression of Kv1.3 and KCa3.1 in third-generation CAR T cells that target the HER2 protein found in specific breast cancer cell types. Initially, we assessed whether the expression of CAR on the surface of human T cells would induce changes in the whole-cell conductance of these two channels. Our results indicated that the conductance of KCa3.1 in third-generation CAR T cells was greater than that in control cells, while Kv1.3 conductance remained unchanged. These findings clearly demonstrate that the expression of this ion channel is not inhibited by the introduction of CAR into $CD3^+$ cells, suggesting that the effector function and Ca^{2+}-dependent signaling remain unaffected by significant alterations in the expression of these channels. Moreover, the heightened activity of KCa3.1 may enhance the chemokine-driven migratory ability of CAR cells, potentially aiding their penetration into tumors[181].

It is generally recognized that $CD8^+$ CAR T cells exhibit greater killing efficacy due to their elevated lytic activity [182] . Consequently, we evaluated the expression of ion channels in third-generation CAR T cells, specifically $CD4^+$ and $CD8^+$ populations: the $CD8^+$ CAR T cells displayed significantly higher levels of KCa3.1, whereas the $CD4^+$ cells showed no notable changes in the expression of either KCa3.1 or Kv1.3 when compared to the corresponding NT control group (Figure19 A and B). Nonetheless, it is worth noting that KCa3.1 conductance was also increased in $CD4^+$ CARs relative to NT cells, although this difference was not statistically significant. Previous studies have indicated that KCa3.1 in $CD8^+$ T cells is involved in chemokine gradient-induced migration[182] , which may direct them towards the tumor site. We believe that this enhanced activity of KCa3.1 could promote the infiltration of $CD8^+$ CAR T cells into solid tumors, resulting in a favorable therapeutic outcome. Additionally, it has been demonstrated that the anti-tumor cytotoxicity of CAR T cells correlates with the cytokine/chemokine profile[183]. We propose that ion channels may play a role in these activated pathways, underscoring the necessity for further research.

Subsequently, we examined the Ca^{2+}-response in CAR T cells: the cytosolic Ca^{2+} concentration is regarded as a vital trigger for regulating a variety of effector functions. The influx of Ca^{2+} through the CRAC channel is modulated by the coordinated activity of ion channels within the T cell membrane; therefore, we opted for thapsigargin-induced activation of CRAC, which circumvents the TCR/CD3 activation pathway and offers direct evidence of ion channel regulation of the Ca^{2+}-response. In our present research, we explored whether the expression of

the anti-HER2 CAR would affect the Ca^{2+}-response. Our findings indicate that in the case of $CD8^+$ CAR T cells, the Ca^{2+} influx is diminished compared to $CD8^+$ NT cells. Conversely, $CD4^+$ CAR and NT T cells exhibited similar Ca^{2+} signaling triggered by the Ca^{2+} release from the ER. Given that the expression of KCa3.1 was elevated in CD8 CARs, potentially leading to increased SOCE, we hypothesize that the expression of CRAC (ORAI1 and STIM1) should be lower in $CD8^+$ CAR T cells.

Finally, we investigated whether the inhibition of K^+ channels (Kv1.3 and KCa3.1) affects the efficacy of $CD8^+$ CAR T cells in killing target cells. Prior research indicated that TRAM-34 effectively inhibits both the native and cloned KCa3.1 channels in human T lymphocytes (K_d of 20–25 nM) and is 200 to 1500-fold more selective than other ion channels [30]. Additionally, Vm24, with a K_d of approximately 3 pM, shows a high selectivity for Kv1.3 channel [184].Our findings revealed that a decrease in Kv1.3 channel conductance (achieved by nearly completely blocking the channels with an approximate 300-fold K_d of Vm24) enhanced the CAR T cells' killing efficiency. Furthermore, antagonizing KCa3.1 channels also aided in the elimination of $HER2^+$ cells. Although one might expect that blocking KCa3.1 and Kv1.3 channels would hinder CTL function, this assumption may not hold true for CTLs and NKs. Previous studies demonstrated that inhibiting KCa3.1 with TRAM-34 in natural killer (NK) cells leads to plasma membrane depolarization, which boosts their cytotoxicity and degranulation against target cells. Nevertheless, this blockade did not impact their migratory capabilities or chemokine expression [185]. A recent research has indicated that specific inhibition of KCa3.1/Kv1.3 channels, which reduces calcium entry (SOCE), enhances NK cell cytotoxicity against the T-ALL Jurkat cell line [186]. It has also been reported that effective target cell killing necessitates an optimal intracellular Ca^{2+} concentration, which can be achieved by impairing the functional expression of CRAC [187]. Given the availability of highly potent and selective blockers, as well as molecular biology tools to modulate the expression of these K^+ channels, we believe that their modification could pave the way for new approaches in CAR T cell therapy.

It is important to mention that our study has certain limitations. Firstly, the signaling pathway, which can be altered with the introduction of the CAR. This requires further investigation to understand the impact of CAR expression such as cytokine production and cell migration. Secondly, the effectiveness of the channel blockers used in this study needs to be assessed i*n vivo*, primary due to the inhibitory nature of the tumor microenvironment.

Here we showed that inhibition of Kv1.3 conductivity with a specific blocker (Vm24) could result in an increased killing rate for CAR-T cells derived from primary $CD8^+$ T cells (long (24-hour) period), which also express KCa3.1, another channel essential for Ca^{2+}-dependent

functions [175]. However, for Jurkat-CAR model we obtained that prevention of the Kv1.3 channel redistribution impaired the killing potential (short (3-hour) period). To explain this discrepancy, we must mention that Jurkat cells lack KCa3.1, which could otherwise compensate for the absence of Kv1.3 function in T cells; thus, the killing of target cells may be hindered, at least during the initial phase or short duration [178, 188].

7 SUMMARY

T cell ion channels (Kv1.3, KCa3.1 and CRAC) regulate the activation and effector functions via modulating the Ca^{2+}-dependent pathway. Chimeric antigen receptor (CAR T cell therapy) showed a remarkable success in anti-tumor therapy, especially in the treatment of chemotherapy-resistant liquid cancers. Nevertheless, the mechanisms regulating CAR-T cell function as well as the side effects remain an area of active research.

In our research study, we assessed the expression and role of ion channels in CAR T cells using a Jurkat-cell model and in primary T cells.

Our results from molecular, electrophysiological and functional assays highlight that the KCa3.1 conductance in HER2-specific CAR T cells was higher compared to the non-transduced (NT, control) cells, which was more prominent in the $CD8^+$ population ($CD4^+$ cell also showed elevation). The Kv1.3 expression level was the same for all cell types ($CD4^+$, $CD8^+$, CAR, and NT). Single-cell Ca^{2+} imaging revealed that thapsigargin-induced SOCE via CRAC is suppressed in $CD8^+$ CAR T cells, unlike for $CD4^+$ and $CD8^+$ NT cells. The use of specific antagonists (Kv1.3: Vm24; KCa3.1: TRAM-34): showed that the target cell elimination capacity of the $CD8^+$ CAR T cells was improved either by blocking KCa3.1 or Kv1.3.

By means of our Jurkat-CAR cell line we could show that Kv1.3 channels is colocalized with CAR and redistributes into the synapse between a CAR and a target cell. The biophysical properties of Kv1.3 channel are not vastly affected by the introduction of CAR in the cells when Kv1.3 is the only expressed channel. The blockage of Kv1.3 channel lateral movement to the synapse affects the killing potential of CAR-T cells, likely through disruption of the Ca^{2+}-response upon IS formation. Overall, these data suggest that the manipulation of the Kv1.3 channel may contribute to the improvement of CAR-T immunotherapy and provide new insights for future clinical strategies.

8 REFERENCES

1. Subramanyam, P. and H.M. Colecraft, *Ion channel engineering: perspectives and strategies.* J Mol Biol, 2015. 427(1): p. 190-204.
2. Gadsby, D.C., *Ion channels versus ion pumps: the principal difference, in principle.* Nature Reviews Molecular Cell Biology, 2009. 10(5): p. 344-352.
3. Dai, G., *Signaling by Ion Channels: Pathways, Dynamics and Channelopathies.* Mo Med, 2023. 120(5): p. 367-373.
4. Benarroch, E.E., *Potassium channels: brief overview and implications in epilepsy.* Neurology, 2009. 72(7): p. 664-9.
5. Rader, R.K., et al., *T cell activation is regulated by voltage-dependent and calcium-activated potassium channels.* The Journal of Immunology, 1996. 156(4): p. 1425-1430.
6. Wei, A., T. Jegla, and L. Salkoff, *Eight Potassium Channel Families Revealed by the C. elegans Genome Project.* Neuropharmacology, 1996. 35(7): p. 805-829.
7. Grover, G.J. and K.D. Garlid, *ATP-Sensitive Potassium Channels: A Review of their Cardioprotective Pharmacology.* Journal of Molecular and Cellular Cardiology, 2000. 32(4): p. 677-695.
8. Ryoo, K. and J.Y. Park, *Two-pore Domain Potassium Channels in Astrocytes.* Exp Neurobiol, 2016. 25(5): p. 222-232.
9. Stephen PH Alexander , E.K., Alistair Mathie , John A Peters, Emma L Veale , Jane F Armstrong ,, et al., *THE CONCISE GUIDE TO PHARMACOLOGY 2019/20: Introduction and Other Protein Targets.* British journal of pharmacology, 2019(176): p. S1-S20.
10. Heginbotham, L., et al., *Mutations in the K+ channel signature sequence.* Biophys J, 1994. 66(4): p. 1061-7.
11. Chou, K.-C., *Insights from Modeling Three-Dimensional Structures of the Human Potassium and Sodium Channels.* Journal of Proteome Research, 2004. 3(4): p. 856-861.
12. González, C., et al., *K(+) channels: function-structural overview.* Compr Physiol, 2012. 2(3): p. 2087-149.
13. Harmar, A.J., et al., *IUPHAR-DB: the IUPHAR database of G protein-coupled receptors and ion channels.* Nucleic Acids Res, 2009. 37(Database issue): p. D680-5.
14. Jiang, Y., et al., *X-ray structure of a voltage-dependent K+ channel.* Nature, 2003. 423(6935): p. 33-41.
15. Long, S.B., E.B. Campbell, and R. Mackinnon, *Voltage sensor of Kv1.2: structural basis of electromechanical coupling.* Science, 2005. 309(5736): p. 903-8.
16. Kubo, Y., et al., *International Union of Pharmacology. LIV. Nomenclature and molecular relationships of inwardly rectifying potassium channels.* Pharmacol Rev, 2005. 57(4): p. 509-26.
17. Gutman, G.A., et al., *International Union of Pharmacology. LIII. Nomenclature and molecular relationships of voltage-gated potassium channels.* Pharmacol Rev, 2005. 57(4): p. 473-508.
18. Rudy, B., Maffie, J., Amarillo, Y., Clark, B., Goldberg, E. M., Jeong, H. Y., Kruglikov, I., Kwon, E., Nadal, M., & Zagha, E., *Voltage Gated Potassium Channels: Structure and Function of Kv1 to Kv9 Subfamilies.* In Encyclopedia of Neuroscience 2009. (pp. 397-425).
19. Wulff, H. and B.S. Zhorov, *K+ channel modulators for the treatment of neurological disorders and autoimmune diseases.* Chem Rev, 2008. 108(5): p. 1744-73.

20. Pérez-García, M.T., P. Cidad, and J.R. López-López, *The secret life of ion channels: Kv1.3 potassium channels and proliferation.* Am J Physiol Cell Physiol, 2018. 314(1): p. C27-c42.
21. Panyi, G., *Biophysical and pharmacological aspects of K+ channels in T lymphocytes.* Eur Biophys J, 2005. 34(6): p. 515-29.
22. Reddi, R., et al., *Structural basis for C-type inactivation in a Shaker family voltage-gated K+ channel.* Science Advances, 2022. 8(16): p. eabm8804.
23. Selvakumar, P., et al., *Structures of the T cell potassium channel Kv1.3 with immunoglobulin modulators.* Nat Commun, 2022. 13(1): p. 3854.
24. Krnjević, K. and A. Lisiewicz, *Injections of calcium ions into spinal motoneurones.* J Physiol, 1972. 225(2): p. 363-90.
25. Ghatta, S., et al., *Large-conductance, calcium-activated potassium channels: Structural and functional implications.* Pharmacology & Therapeutics, 2006. 110(1): p. 103-116.
26. Xia, X.M., et al., *Mechanism of calcium gating in small-conductance calcium-activated potassium channels.* Nature, 1998. 395(6701): p. 503-507.
27. Marty, A., *Ca-dependent K channels with large unitary conductance in chromaffin cell membranes.* Nature, 1981. 291(5815): p. 497-500.
28. Sweet, T.B. and D.H. Cox, *Measurements of the BKCa channel's high-affinity Ca2+ binding constants: effects of membrane voltage.* J Gen Physiol, 2008. 132(5): p. 491-505.
29. Brown, B.M., et al., *Pharmacology of Small- and Intermediate-Conductance Calcium-Activated Potassium Channels.* Annu Rev Pharmacol Toxicol, 2020. 60: p. 219-240.
30. Xia, X.M., et al., *Mechanism of calcium gating in small-conductance calcium-activated potassium channels.* Nature, 1998. 395(6701): p. 503-7.
31. Wei, A., et al., *Calcium sensitivity of BK-type KCa channels determined by a separable domain.* Neuron, 1994. 13(3): p. 671-81.
32. Thiel, G. and O.G. Rössler, *Calmodulin Regulates Transient Receptor Potential TRPM3 and TRPM8-Induced Gene Transcription.* International Journal of Molecular Sciences, 2023. 24(9): p. 7902.
33. Kovalenko, I., et al., *Identification of KCa3.1 Channel as a Novel Regulator of Oxidative Phosphorylation in a Subset of Pancreatic Carcinoma Cell Lines.* PLOS ONE, 2016. 11(8): p. e0160658.
34. Lam, J., et al., *The therapeutic potential of small-conductance KCa2 channels in neurodegenerative and psychiatric diseases.* Expert Opinion on Therapeutic Targets, 2013. 17: p. 1203 - 1220.
35. Fanger, C.M., et al., *Calmodulin Mediates Calcium-dependent Activation of the Intermediate Conductance KCa Channel,IKCa1 *.* Journal of Biological Chemistry, 1999. 274(9): p. 5746-5754.
36. Ghanshani, S., et al., *Up-regulation of the IKCa1 potassium channel during T-cell activation. Molecular mechanism and functional consequences.* J Biol Chem, 2000. 275(47): p. 37137-49.
37. Feske, S., H. Wulff, and E.Y. Skolnik, *Ion channels in innate and adaptive immunity.* Annu Rev Immunol, 2015. 33: p. 291-353.
38. Dong, D.-L., Y.-L. Bai, and B.-Z. Cai, *Chapter Six - Calcium-Activated Potassium Channels: Potential Target for Cardiovascular Diseases*, in *Advances in Protein Chemistry and Structural Biology*, R. Donev, Editor. 2016, Academic Press. p. 233-261.
39. Figueiredo, I.A.D., et al., *A review of the pathophysiology and the role of ion channels on bronchial asthma.* Front Pharmacol, 2023. 14: p. 1236550.

40. Berridge, M.J., *Capacitative calcium entry.* Biochem J, 1995. 312 (Pt 1)(Pt 1): p. 1-11.
41. Lewis, R.S., *Calcium signaling mechanisms in T lymphocytes.* Annu Rev Immunol, 2001. 19: p. 497-521.
42. Parekh, A.B. and J.W. Putney, Jr., *Store-operated calcium channels.* Physiol Rev, 2005. 85(2): p. 757-810.
43. Lewis, R.S., *The molecular choreography of a store-operated calcium channel.* Nature, 2007. 446(7133): p. 284-287.
44. Feske, S., et al., *A mutation in Orai1 causes immune deficiency by abrogating CRAC channel function.* Nature, 2006. 441(7090): p. 179-185.
45. Roos, J., et al., *STIM1, an essential and conserved component of store-operated Ca2+ channel function.* J Cell Biol, 2005. 169(3): p. 435-45.
46. Zhang, S.L., et al., *Genome-wide RNAi screen of Ca(2+) influx identifies genes that regulate Ca(2+) release-activated Ca(2+) channel activity.* Proc Natl Acad Sci U S A, 2006. 103(24): p. 9357-62.
47. Parekh, A.B., *Store-operated CRAC channels: function in health and disease.* Nature Reviews Drug Discovery, 2010. 9(5): p. 399-410.
48. Motiani, R.K., I.F. Abdullaev, and M. Trebak, *A Novel Native Store-operated Calcium Channel Encoded by Orai3: selective requirement of orai3 versus orai1 in estrogen receptor-positive versus estrogen receptor-negative breast cancer cells *.* Journal of Biological Chemistry, 2010. 285(25): p. 19173-19183.
49. Sutovska, M., et al. *CRAC Ion Channels and Airway Defense Reflexes in Experimental Allergic Inflammation*. in *Respiratory Regulation - The Molecular Approach*. 2013. Dordrecht: Springer Netherlands.
50. Parkin, J. and B. Cohen, *An overview of the immune system.* The Lancet, 2001. 357(9270): p. 1777-1789.
51. Nicholson, Lindsay B., *The immune system.* Essays in Biochemistry, 2016. 60(3): p. 275-301.
52. Yatim, K.M. and F.G. Lakkis, *A Brief Journey through the Immune System.* Clinical Journal of the American Society of Nephrology, 2015. 10(7).
53. DeCoursey, T.E., et al., *Voltage-dependent ion channels in T-lymphocytes.* J Neuroimmunol, 1985. 10(1): p. 71-95.
54. Matteson, D.R. and C. Deutsch, *K channels in T lymphocytes: a patch clamp study using monoclonal antibody adhesion.* Nature, 1984. 307(5950): p. 468-471.
55. Grissmer, S., et al., *Expression and chromosomal localization of a lymphocyte K+ channel gene.* Proc Natl Acad Sci U S A, 1990. 87(23): p. 9411-5.
56. Krabbendam, I.E., et al., *Mitochondrial Ca2+-activated K+ channels and their role in cell life and death pathways.* Cell Calcium, 2018. 69: p. 101-111.
57. Kuum, M., V. Veksler, and A. Kaasik, *Potassium fluxes across the endoplasmic reticulum and their role in endoplasmic reticulum calcium homeostasis.* Cell Calcium, 2015. 58(1): p. 79-85.
58. Kim, J.B., *Channelopathies.* Korean J Pediatr, 2014. 57(1): p. 1-18.
59. Fanger, C.M., et al., *Characterization of T cell mutants with defects in capacitative calcium entry: genetic evidence for the physiological roles of CRAC channels.* J Cell Biol, 1995. 131(3): p. 655-67.
60. Feske, S., et al., *Gene regulation mediated by calcium signals in T lymphocytes.* Nat Immunol, 2001. 2(4): p. 316-24.
61. Le Deist, F., et al., *A primary T-cell immunodeficiency associated with defective transmembrane calcium influx.* Blood, 1995. 85(4): p. 1053-62.

62. Partiseti, M., et al., *The calcium current activated by T cell receptor and store depletion in human lymphocytes is absent in a primary immunodeficiency.* J Biol Chem, 1994. 269(51): p. 32327-35.
63. Schwarz, A., et al., *Ca2+ Signaling in Identified T-lymphocytes from Human Intestinal Mucosa: RELATION TO HYPOREACTIVITY, PROLIFERATION, AND INFLAMMATORY BOWEL DISEASE **.* Journal of Biological Chemistry, 2004. 279(7): p. 5641-5647.
64. Wang, J. and M. Xiang, *Targeting Potassium Channels Kv1.3 and Ka3.1: Routes to Selective Immunomodulators in Autoimmune Disorder Treatment?* Pharmacotherapy: The Journal of Human Pharmacology and Drug Therapy, 2013. 33(5): p. 515-528.
65. Cahalan, M.D. and K.G. Chandy, *The functional network of ion channels in T lymphocytes.* Immunological Reviews, 2009. 231(1): p. 59-87.
66. Feske, S., E.Y. Skolnik, and M. Prakriya, *Ion channels and transporters in lymphocyte function and immunity.* Nat Rev Immunol, 2012. 12(7): p. 532-47.
67. Beeton, C., et al., *Kv1.3 channels are a therapeutic target for T cell-mediated autoimmune diseases.* Proc Natl Acad Sci U S A, 2006. 103(46): p. 17414-9.
68. Wulff, H., et al., *The voltage-gated Kv1.3 K(+) channel in effector memory T cells as new target for MS.* J Clin Invest, 2003. 111(11): p. 1703-13.
69. Chimote, A.A., et al., *A Compartmentalized Reduction in Membrane-Proximal Calmodulin Reduces the Immune Surveillance Capabilities of CD8(+) T Cells in Head and Neck Cancer.* Front Pharmacol, 2020. 11: p. 143.
70. Witz, I.P. and O. Levy-Nissenbaum, *The tumor microenvironment in the post-PAGET era.* Cancer Lett, 2006. 242(1): p. 1-10.
71. Tuccitto, A., et al., *Immunosuppressive circuits in tumor microenvironment and their influence on cancer treatment efficacy.* Virchows Arch, 2019. 474(4): p. 407-420.
72. Blay, J., T.D. White, and D.W. Hoskin, *The extracellular fluid of solid carcinomas contains immunosuppressive concentrations of adenosine.* Cancer Res, 1997. 57(13): p. 2602-5.
73. Hoskin, D.W., et al., *Adenosine acts through an A3 receptor to prevent the induction of murine anti-CD3-activated killer T cells.* Int J Cancer, 2002. 99(3): p. 386-95.
74. Linden, J., *Adenosine metabolism and cancer. Focus on "Adenosine downregulates DPPIV on HT-29 colon cancer cells by stimulating protein tyrosine phosphatases and reducing ERK1/2 activity via a novel pathway".* Am J Physiol Cell Physiol, 2006. 291(3): p. C405-6.
75. Antonioli, L., et al., *Immunity, inflammation and cancer: a leading role for adenosine.* Nat Rev Cancer, 2013. 13(12): p. 842-57.
76. Chimote, A.A., et al., *Selective inhibition of KCa3.1 channels mediates adenosine regulation of the motility of human T cells.* J Immunol, 2013. 191(12): p. 6273-80.
77. Chandy, K.G. and R.S. Norton, *Peptide blockers of Kv1.3 channels in T cells as therapeutics for autoimmune disease.* Current Opinion in Chemical Biology, 2017. 38: p. 97-107.
78. Shen, B., et al., *Treating autoimmune disorders with venom-derived peptides.* Expert Opinion on Biological Therapy, 2017. 17(9): p. 1065-1075.
79. Varga, Z., et al., *Potassium channel expression in human CD4+ regulatory and naïve T cells from healthy subjects and multiple sclerosis patients.* Immunology Letters, 2009. 124(2): p. 95-101.
80. George Chandy, K., et al., *K+ channels as targets for specific immunomodulation.* Trends in Pharmacological Sciences, 2004. 25(5): p. 280-289.

81. Schmitz, A., et al., *Design of PAP-1, a Selective Small Molecule Kv1.3 Blocker, for the Suppression of Effector Memory T Cells in Autoimmune Diseases.* Molecular Pharmacology, 2005. 68(5): p. 1254-1270.
82. Gubič, Š., et al., *Discovery of KV1.3 ion channel inhibitors: Medicinal chemistry approaches and challenges.* Medicinal Research Reviews, 2021. 41(4): p. 2423-2473.
83. Tabakmakher, V.M., et al., *Kalium 2.0, a comprehensive database of polypeptide ligands of potassium channels.* Scientific Data, 2019. 6(1): p. 73.
84. Borrego, J., et al., *Recombinant Expression in Pichia pastoris System of Three Potent Kv1.3 Channel Blockers: Vm24, Anuroctoxin, and Ts6.* Journal of Fungi, 2022. 8(11): p. 1215.
85. Varga, Z., et al., *Vm24, a Natural Immunosuppressive Peptide, Potently and Selectively Blocks Kv1.3 Potassium Channels of Human T Cells.* Molecular Pharmacology, 2012. 82(3): p. 372-382.
86. Veytia-Bucheli, J.I., et al., *Kv1.3 channel blockade with the Vm24 scorpion toxin attenuates the CD4+ effector memory T cell response to TCR stimulation.* Cell Communication and Signaling, 2018. 16(1): p. 45.
87. Cs. Szabo, B., et al., *Novel insights into the modulation of the voltage-gated potassium channel Kv1.3 activation gating by membrane ceramides.* Journal of Lipid Research, 2024. 65(8).
88. Wulff, H. and N.A. and Castle, *Therapeutic potential of KCa3.1 blockers: recent advances and promising trends.* Expert Review of Clinical Pharmacology, 2010. 3(3): p. 385-396.
89. Stocker, J.W., et al., *ICA-17043, a novel Gardos channel blocker, prevents sickled red blood cell dehydration in vitro and in vivo in SAD mice.* Blood, 2003. 101(6): p. 2412-8.
90. Brown, B.M., B. Pressley, and H. Wulff, *KCa3.1 Channel Modulators as Potential Therapeutic Compounds for Glioblastoma.* Curr Neuropharmacol, 2018. 16(5): p. 618-626.
91. Kaushal, V., et al., *The Ca²⁺-Activated K⁺ Channel KCNN4/KCa3.1 Contributes to Microglia Activation and Nitric Oxide-Dependent Neurodegeneration.* The Journal of Neuroscience, 2007. 27(1): p. 234-244.
92. Wang, Z.H., et al., *Blockage of intermediate-conductance-Ca2+-activated K+ channels inhibits progression of human endometrial cancer.* Oncogene, 2007. 26(35): p. 5107-5114.
93. Grgic, I., et al., *Blockade of T-Lymphocyte KCa3.1 and Kv1.3 Channels as Novel Immunosuppression Strategy to Prevent Kidney Allograft Rejection.* Transplantation Proceedings, 2009. 41(6): p. 2601-2606.
94. Cuthbert, A.W., et al., *Activation of Ca(2+)- and cAMP-sensitive K(+) channels in murine colonic epithelia by 1-ethyl-2-benzimidazolone.* Am J Physiol, 1999. 277(1): p. C111-20.
95. Anderson, N.J., S. Slough, and W.P. Watson, *In vivo characterisation of the small-conductance KCa (SK) channel activator 1-ethyl-2-benzimidazolinone (1-EBIO) as a potential anticonvulsant.* European Journal of Pharmacology, 2006. 546(1): p. 48-53.
96. Strøbæk, D., et al., *Activation of human IK and SK Ca2+-activated K+ channels by NS309 (6,7-dichloro-1H-indole-2,3-dione 3-oxime).* Biochimica et Biophysica Acta (BBA) - Biomembranes, 2004. 1665(1): p. 1-5.
97. Shaw, A.S. and M.L. Dustin, *Making the T cell receptor go the distance: a topological view of T cell activation.* Immunity, 1997. 6(4): p. 361-9.
98. Davis, S.J. and P.A. van der Merwe, *The kinetic-segregation model: TCR triggering and beyond.* Nat Immunol, 2006. 7(8): p. 803-9.

99. Negulescu, P.A., et al., *Polarity of T cell shape, motility, and sensitivity to antigen.* Immunity, 1996. 4(5): p. 421-30.
100. Quintana, A., et al., *Morphological changes of T cells following formation of the immunological synapse modulate intracellular calcium signals.* Cell Calcium, 2009. 45(2): p. 109-22.
101. Faure, S., et al., *ERM proteins regulate cytoskeleton relaxation promoting T cell-APC conjugation.* Nat Immunol, 2004. 5(3): p. 272-9.
102. van der Merwe, P.A., *Formation and function of the immunological synapse.* Curr Opin Immunol, 2002. 14(3): p. 293-8.
103. Grakoui, A., et al., *The immunological synapse: a molecular machine controlling T cell activation.* Science, 1999. 285(5425): p. 221-7.
104. Bromley, S.K., et al., *The immunological synapse.* Annu Rev Immunol, 2001. 19: p. 375-96.
105. Nicolaou, S.A., et al., *The Ca(2+)-activated K(+) channel KCa3.1 compartmentalizes in the immunological synapse of human T lymphocytes.* Am J Physiol Cell Physiol, 2007. 292(4): p. C1431-9.
106. Nicolaou, S.A., et al., *Altered Dynamics of Kv1.3 Channel Compartmentalization in the Immunological Synapse in Systemic Lupus Erythematosus1.* The Journal of Immunology, 2007. 179(1): p. 346-356.
107. Panyi, G., et al., *Kv1.3 potassium channels are localized in the immunological synapse formed between cytotoxic and target cells.* Proceedings of the National Academy of Sciences, 2004. 101(5): p. 1285-1290.
108. Nicolaou, S.A., et al., *Localization of Kv1.3 Channels in the Immunological Synapse Modulates the Calcium Response to Antigen Stimulation in T Lymphocytes1.* The Journal of Immunology, 2009. 183(10): p. 6296-6302.
109. Uscanga-Palomeque, A.C., et al., *CAR-T Cell Therapy: From the Shop to Cancer Therapy.* Int J Mol Sci, 2023. 24(21).
110. Ren, J., et al., *Multiplex Genome Editing to Generate Universal CAR T Cells Resistant to PD1 Inhibition.* Clin Cancer Res, 2017. 23(9): p. 2255-2266.
111. Guercio, M., et al., *Inclusion of the Inducible Caspase 9 Suicide Gene in CAR Construct Increases Safety of CAR.CD19 T Cell Therapy in B-Cell Malignancies.* Front Immunol, 2021. 12: p. 755639.
112. Chmielewski, M., A.A. Hombach, and H. Abken, *Of CARs and TRUCKs: chimeric antigen receptor (CAR) T cells engineered with an inducible cytokine to modulate the tumor stroma.* Immunol Rev, 2014. 257(1): p. 83-90.
113. Hong, M., J.D. Clubb, and Y.Y. Chen, *Engineering CAR-T Cells for Next-Generation Cancer Therapy.* Cancer Cell, 2020. 38(4): p. 473-488.
114. Thomas, S. and H. Abken, *CAR T cell therapy becomes CHIC: "cytokine help intensified CAR" T cells.* Front Immunol, 2022. 13: p. 1090959.
115. Urbanska, K., et al., *A universal strategy for adoptive immunotherapy of cancer through use of a novel T-cell antigen receptor.* Cancer Res, 2012. 72(7): p. 1844-52.
116. Cho, J.H., J.J. Collins, and W.W. Wong, *Universal Chimeric Antigen Receptors for Multiplexed and Logical Control of T Cell Responses.* Cell, 2018. 173(6): p. 1426-1438.e11.
117. Abou-El-Enein, M., et al., *Scalable Manufacturing of CAR T cells for Cancer Immunotherapy.* Blood Cancer Discov, 2021. 2(5): p. 408-422.
118. Golubovskaya, V. and L. Wu, *Different Subsets of T Cells, Memory, Effector Functions, and CAR-T Immunotherapy.* Cancers (Basel), 2016. 8(3).

119. Abken, H., M. Chmielewski, and A.A. Hombach, *Antigen-Specific T-Cell Activation Independently of the MHC: Chimeric Antigen Receptor-Redirected T Cells.* Frontiers in Immunology, 2013. Volume 4 - 2013.
120. Berger, C., et al., *Adoptive transfer of effector CD8+ T cells derived from central memory cells establishes persistent T cell memory in primates.* J Clin Invest, 2008. 118(1): p. 294-305.
121. Kumamoto, Y., et al., *CD4+ T cells support cytotoxic T lymphocyte priming by controlling lymph node input.* Proc Natl Acad Sci U S A, 2011. 108(21): p. 8749-54.
122. Bos, R. and L.A. Sherman, *CD4+ T-cell help in the tumor milieu is required for recruitment and cytolytic function of CD8+ T lymphocytes.* Cancer Res, 2010. 70(21): p. 8368-77.
123. Sommermeyer, D., et al., *Chimeric antigen receptor-modified T cells derived from defined CD8+ and CD4+ subsets confer superior antitumor reactivity in vivo.* Leukemia, 2016. 30(2): p. 492-500.
124. Levine, B.L., et al., *Effects of CD28 costimulation on long-term proliferation of CD4+ T cells in the absence of exogenous feeder cells.* J Immunol, 1997. 159(12): p. 5921-30.
125. Maus, M.V., et al., *Ex vivo expansion of polyclonal and antigen-specific cytotoxic T lymphocytes by artificial APCs expressing ligands for the T-cell receptor, CD28 and 4-1BB.* Nat Biotechnol, 2002. 20(2): p. 143-8.
126. Rubinstein, M.P., et al., *IL-7 and IL-15 differentially regulate CD8+ T-cell subsets during contraction of the immune response.* Blood, 2008. 112(9): p. 3704-12.
127. Alizadeh, D., et al., *IL15 Enhances CAR-T Cell Antitumor Activity by Reducing mTORC1 Activity and Preserving Their Stem Cell Memory Phenotype.* Cancer Immunol Res, 2019. 7(5): p. 759-772.
128. Poorebrahim, M., et al., *Production of CAR T-cells by GMP-grade lentiviral vectors: latest advances and future prospects.* Critical Reviews in Clinical Laboratory Sciences, 2019. 56(6): p. 393-419.
129. Dimitri, A., F. Herbst, and J.A. Fraietta, *Engineering the next-generation of CAR T-cells with CRISPR-Cas9 gene editing.* Mol Cancer, 2022. 21(1): p. 78.
130. Larson, R.C. and M.V. Maus, *Recent advances and discoveries in the mechanisms and functions of CAR T cells.* Nat Rev Cancer, 2021. 21(3): p. 145-161.
131. Ayala Ceja, M., et al., *CAR-T cell manufacturing: Major process parameters and next-generation strategies.* J Exp Med, 2024. 221(2).
132. Kochenderfer, J.N., et al., *Eradication of B-lineage cells and regression of lymphoma in a patient treated with autologous T cells genetically engineered to recognize CD19.* Blood, 2010. 116(20): p. 4099-102.
133. Porter, D.L., et al., *Chimeric antigen receptor-modified T cells in chronic lymphoid leukemia.* N Engl J Med, 2011. 365(8): p. 725-33.
134. Ong, M.Z., et al., *FDA-approved CAR T-cell Therapy: A Decade of Progress and Challenges.* Curr Pharm Biotechnol, 2024. 25(11): p. 1377-1393.
135. Chekmasova, A.A., et al., *Successful eradication of established peritoneal ovarian tumors in SCID-Beige mice following adoptive transfer of T cells genetically targeted to the MUC16 antigen.* Clin Cancer Res, 2010. 16(14): p. 3594-606.
136. Zhou, R., et al., *CAR T Cells Targeting the Tumor MUC1 Glycoprotein Reduce Triple-Negative Breast Cancer Growth.* Front Immunol, 2019. 10: p. 1149.
137. Slovin, S.F., et al., *Chimeric antigen receptor CAR modified T cells targeting prostate-specific membrane antigen (PSMA) in patients (pts) with castrate metastatic prostate cancer (CMPC).* Journal of Clinical Oncology, 2013. 31(6_suppl): p. 72-72.

138. Whilding, L.M., et al., *CAR T-Cells Targeting the Integrin αvβ6 and Co-Expressing the Chemokine Receptor CXCR2 Demonstrate Enhanced Homing and Efficacy against Several Solid Malignancies.* Cancers (Basel), 2019. 11(5).
139. Wallstabe, L., et al., *ROR1-CAR T cells are effective against lung and breast cancer in advanced microphysiologic 3D tumor models.* JCI Insight, 2019. 4(18).
140. Batra, S.A., et al., *Glypican-3-Specific CAR T Cells Coexpressing IL15 and IL21 Have Superior Expansion and Antitumor Activity against Hepatocellular Carcinoma.* Cancer Immunol Res, 2020. 8(3): p. 309-320.
141. Zhang, E., J. Gu, and H. Xu, *Prospects for chimeric antigen receptor-modified T cell therapy for solid tumors.* Mol Cancer, 2018. 17(1): p. 7.
142. Khan, J.F., A.S. Khan, and R.J. Brentjens, *Chapter Eight - Application of CAR T cells for the treatment of solid tumors*, in *Progress in Molecular Biology and Translational Science*, D.B. Teplow, Editor. 2019, Academic Press. p. 293-327.
143. Salmon, H., et al., *Matrix architecture defines the preferential localization and migration of T cells into the stroma of human lung tumors.* J Clin Invest, 2012. 122(3): p. 899-910.
144. Vedvyas, Y., et al., *Manufacturing and preclinical validation of CAR T cells targeting ICAM-1 for advanced thyroid cancer therapy.* Sci Rep, 2019. 9(1): p. 10634.
145. Poznansky, M.C., et al., *Thymocyte emigration is mediated by active movement away from stroma-derived factors.* J Clin Invest, 2002. 109(8): p. 1101-10.
146. Sridhar, P. and F. Petrocca, *Regional Delivery of Chimeric Antigen Receptor (CAR) T-Cells for Cancer Therapy.* Cancers, 2017. 9(7): p. 92.
147. Quail, D.F. and J.A. Joyce, *Microenvironmental regulation of tumor progression and metastasis.* Nat Med, 2013. 19(11): p. 1423-37.
148. Laetsch, T.W., et al., *Three-Year Update of Tisagenlecleucel in Pediatric and Young Adult Patients With Relapsed/Refractory Acute Lymphoblastic Leukemia in the ELIANA Trial.* J Clin Oncol, 2023. 41(9): p. 1664-1669.
149. Kochenderfer, J.N., et al., *Chemotherapy-refractory diffuse large B-cell lymphoma and indolent B-cell malignancies can be effectively treated with autologous T cells expressing an anti-CD19 chimeric antigen receptor.* J Clin Oncol, 2015. 33(6): p. 540-9.
150. Kansal, R., et al., *Sustained B cell depletion by CD19-targeted CAR T cells is a highly effective treatment for murine lupus.* Science Translational Medicine, 2019. 11(482): p. eaav1648.
151. Jin, X., et al., *Therapeutic efficacy of anti-CD19 CAR-T cells in a mouse model of systemic lupus erythematosus.* Cell Mol Immunol, 2021. 18(8): p. 1896-1903.
152. Mackensen, A., et al., *Anti-CD19 CAR T cell therapy for refractory systemic lupus erythematosus.* Nat Med, 2022. 28(10): p. 2124-2132.
153. Bergmann, C., et al., *Treatment of a patient with severe systemic sclerosis (SSc) using CD19-targeted CAR T cells.* Ann Rheum Dis, 2023. 82(8): p. 1117-1120.
154. Merkt, W., et al., *Third-generation CD19.CAR-T cell-containing combination therapy in Scl70+ systemic sclerosis.* Annals of the Rheumatic Diseases, 2024. 83(4): p. 543-546.
155. Feng, J., et al., *Safety and Efficacy of CD19 CAR-T Cells for Refractory Systemic Sclerosis: A Phase I Clinical Trial.* Blood, 2022. 140(Supplement 1): p. 10335-10336.
156. Pecher, A.C., et al., *CD19-Targeting CAR T Cells for Myositis and Interstitial Lung Disease Associated With Antisynthetase Syndrome.* Jama, 2023. 329(24): p. 2154-2162.
157. Müller, F., et al., *CD19-targeted CAR T cells in refractory antisynthetase syndrome.* Lancet, 2023. 401(10379): p. 815-818.

158. Schett, G., A. Mackensen, and D. Mougiakakos, *CAR T-cell therapy in autoimmune diseases.* Lancet, 2023. 402(10416): p. 2034-2044.
159. Müller, F., et al., *CD19 CAR T-Cell Therapy in Autoimmune Disease - A Case Series with Follow-up.* N Engl J Med, 2024. 390(8): p. 687-700.
160. Oh, S., et al., *Precision targeting of autoantigen-specific B cells in muscle-specific tyrosine kinase myasthenia gravis with chimeric autoantibody receptor T cells.* Nat Biotechnol, 2023. 41(9): p. 1229-1238.
161. Tanner, M., et al., *Characterization of a novel cell line established from a patient with Herceptin-resistant breast cancer.* Mol Cancer Ther, 2004. 3(12): p. 1585-92.
162. Csaplár, M., et al., *Cytolytic Activity of CAR T Cells and Maintenance of Their CD4+ Subset Is Critical for Optimal Antitumor Activity in Preclinical Solid Tumor Models.* Cancers (Basel), 2021. 13(17).
163. Ahmed, N., et al., *Immunotherapy for osteosarcoma: genetic modification of T cells overcomes low levels of tumor antigen expression.* Mol Ther, 2009. 17(10): p. 1779-87.
164. Mata, M., et al., *Inducible Activation of MyD88 and CD40 in CAR T Cells Results in Controllable and Potent Antitumor Activity in Preclinical Solid Tumor Models.* Cancer Discov, 2017. 7(11): p. 1306-1319.
165. Hamill, O.P., et al., *Improved patch-clamp techniques for high-resolution current recording from cells and cell-free membrane patches.* Pflugers Arch, 1981. 391(2): p. 85-100.
166. Matteson, D.R. and C. Deutsch, *K channels in T lymphocytes: a patch clamp study using monoclonal antibody adhesion.* Nature, 1984. 307(5950): p. 468-71.
167. Kummerow, C., et al., *A simple, economic, time-resolved killing assay.* European Journal of Immunology, 2014. 44(6): p. 1870-1872.
168. Capera, J., et al., *Dynamics and spatial organization of Kv1.3 at the immunological synapse of human CD4+ T cells.* Biophys J, 2024. 123(15): p. 2271-2281.
169. Dong, R., et al., *Rewired signaling network in T cells expressing the chimeric antigen receptor (CAR).* Embo j, 2020. 39(16): p. e104730.
170. Nicolaou, S.A., et al., *Localization of Kv1.3 channels in the immunological synapse modulates the calcium response to antigen stimulation in T lymphocytes.* J Immunol, 2009. 183(10): p. 6296-302.
171. Voros, O., G. Panyi, and P. Hajdu, *Immune Synapse Residency of Orai1 Alters Ca2+ Response of T Cells.* International Journal of Molecular Sciences, 2021. 22(21): p. 11514.
172. Nicolaou, S.A., et al., *Differential calcium signaling and Kv1.3 trafficking to the immunological synapse in systemic lupus erythematosus.* Cell Calcium, 2010. 47(1): p. 19-28.
173. Hu, L., et al., *Blockade of Kv1.3 potassium channels inhibits differentiation and granzyme B secretion of human CD8+ T effector memory lymphocytes.* PLoS One, 2013. 8(1): p. e54267.
174. Bloemberg, D., et al., *A High-Throughput Method for Characterizing Novel Chimeric Antigen Receptors in Jurkat Cells.* Mol Ther Methods Clin Dev, 2020. 16: p. 238-254.
175. Medyouni, G., et al., *Inhibition of K(+) Channels Affects the Target Cell Killing Potential of CAR T Cells.* Cancers (Basel), 2024. 16(22).
176. Panyi, G., et al., *Looking through ion channels: recharged concepts in T-cell signaling.* Trends Immunol, 2004. 25(11): p. 565-9.
177. Wu, L., et al., *Targeting CAR to the Peptide-MHC Complex Reveals Distinct Signaling Compared to That of TCR in a Jurkat T Cell Model.* Cancers (Basel), 2021. 13(4).

178. Srivastava, S., et al., *The Class II Phosphatidylinositol 3 kinase C2β Is Required for the Activation of the K+ Channel KCa3.1 and CD4 T-Cells.* Molecular Biology of the Cell, 2009. 20(17): p. 3783-3791.
179. Sterner, R.C. and R.M. Sterner, *CAR-T cell therapy: current limitations and potential strategies.* Blood Cancer J, 2021. 11(4): p. 69.
180. Meuth, S.G., et al., *TWIK-related Acid-sensitive K+ Channel 1 (TASK1) and TASK3 Critically Influence T Lymphocyte Effector Functions.* Journal of Biological Chemistry, 2008. 283(21): p. 14559-14570.
181. Chimote, A.A., et al., *A defect in KCa3.1 channel activity limits the ability of CD8⁺ T cells from cancer patients to infiltrate an adenosine-rich microenvironment.* Science Signaling, 2018. 11(527): p. eaaq1616.
182. Galli, E., et al., *The CD4/CD8 ratio of infused CD19-CAR-T is a prognostic factor for efficacy and toxicity.* Br J Haematol, 2023. 203(4): p. 564-570.
183. Valiullina, A.K., et al., *Evaluation of CAR-T Cells' Cytotoxicity against Modified Solid Tumor Cell Lines.* Biomedicines, 2023. 11(2).
184. Varga, Z., et al., *Vm24, a natural immunosuppressive peptide, potently and selectively blocks Kv1.3 potassium channels of human T cells.* Mol Pharmacol, 2012. 82(3): p. 372-82.
185. Koshy, S., et al., *Blocking KCa3.1 channels increases tumor cell killing by a subpopulation of human natural killer lymphocytes.* PLoS One, 2013. 8(10): p. e76740.
186. Olivas-Aguirre, M., et al., *Reduction of Ca2+ Entry by a Specific Block of KCa3.1 Channels Optimizes Cytotoxic Activity of NK Cells against T-ALL Jurkat Cells.* Cells, 2023. 12(16): p. 2065.
187. Zhou, X., et al., *A calcium optimum for cytotoxic T lymphocyte and natural killer cell cytotoxicity.* J Physiol, 2018. 596(14): p. 2681-2698.
188. Chiang, E.Y., et al., *Potassium channels Kv1.3 and KCa3.1 cooperatively and compensatorily regulate antigen-specific memory T cell functions.* Nat Commun, 2017. 8: p. 14644.

9 KEYWORDS

Ion channel
CAR-T cell
Kv1.3
KCa3.1
CRAC
Immunotherapy
Cancer
Calcium-response

10 ACKNOWLEDGEMENT

I would like to express my dearest gratitude to my supervisor, **Dr. Peter Hajdu**, for his guidance, support, experience and knowledge invested in this scientific work.
I would like to thank **Prof. György Panyi** as well, for his support during the 5 years of my PhD.
Special thanks to all of my colleagues and friends in the lab**, Gabriella Serrano and Kashmala Shakeel** , thank you for being part of this journey with all the highs and lows.

I would like to extend my sincere thanks to the staff of the Faculty of Medicine and the Doctoral School of Molecular Medicine for fostering a supportive research environment. I am especially grateful to the Department of Biophysics and Cell Biology for providing well-equipped laboratories and dedicated, highly qualified personnel, especially to our laboratory technicians: **Adrienn Bagosi and Cecilia Nagy** who contributed significantly to the success of my research.

Above all, to my precious family members, to my **beloved mother**, though you are not here to see this moment. You taught me perseverance and the value of education. I dedicate this work to your memory. You are deeply missed, always remembered and forever cherished. **To my father and my lovely brothers**. I would never have done it without your continuous support. Your unconditional love, understanding and encouragement, whether near or far, kept me going.

I dedicate this work to you, with all my love and gratitude.

11 APPENDIX

UNIVERSITY of DEBRECEN

UNIVERSITY AND NATIONAL LIBRARY
UNIVERSITY OF DEBRECEN
H-4002 Egyetem tér 1, Debrecen
Phone: +3652/410-443, email: publikaciok@lib.unideb.hu

Registry number: DEENK/466/2025.PL
Subject: PhD Publication List

Candidate: Ghofrane Medyouni
Doctoral School: Doctoral School of Molecular Medicine

List of publications related to the dissertation

1. **Medyouni, G.**, Vörös, O., Panyi, G., Hajdu, P.: Functional role of Kv1.3 localization in CAR-T cells. *J. Immunol. [Epub ahead of print]*, 2025.
   DOI: http://dx.doi.org/10.1093/jimmun/vkaf199
   IF: 3.4 (2024)
2. **Medyouni, G.**, Vörös, O., Jusztus, V., Panyi, G., Vereb, G., Szöőr, Á., Hajdu, P.: Inhibition of K+ Channels Affects the Target Cell Killing Potential of CAR T Cells. *Cancers (Basel). 16* (22), 1-12, 2024.
   DOI: http://dx.doi.org/10.3390/cancers16223750
   IF: 4.4

List of other publications

3. Jusztus, V., **Medyouni, G.**, Bagosi, A., Lampé, R., Panyi, G., Matolay, O., Maka, E., Krasznai, Z. T., Vörös, O., Hajdu, P.: Activity of Potassium Channels in CD8+ T Lymphocytes: diagnostic and Prognostic Biomarker in Ovarian Cancer? *Int. J. Mol. Sci. 25* (4), 1-8, 2024.
   DOI: http://dx.doi.org/10.3390/ijms25041949
   IF: 4.9

Total IF of journals (all publications): 12,7
Total IF of journals (publications related to the dissertation): 7,8

DEBRECENI EGYETEM Egyetemi és Nemzeti Könyvtár

The Candidate's publication data submitted to the Tudóstér have been validated by DEENK on the basis of the Journal Citation Report (Impact Factor) database.

15 September, 2025